Groundwater potential mapping in Trans Yamuna Region, Prayagraj, using combination of geospatial technologies and AHP method

Swarnim · Jayant Nath Tripathi · Irjesh Sonker · Surya Prakash Tiwari

Abstract In this study, the combination of Remote Sensing and Geographic Information System (GIS) was utilized to identify the Groundwater Potential Zones (GPZs) of the Trans-Yamuna region. The Groundwater Potential Zones (GPZ) were mapped by integrating drainage density, slope, geology, geomorphology, NDVI, lineament density, rainfall, soil types, land use & land cover, and topographic wetness index maps. For the prediction output to have a non-trivial degree of accuracy, multicollinearity tests were run before integrating the layers. Using the Analytical Hierarchy Process (AHP), groundwater recharge-affecting parameters and classes of each parameter were scored. All thematic layers were integrated using weighted linear combination on a GIS platform to create a groundwater potential zone map. The outcomes of the model indicate that the research region exhibits three distinct groundwater potential zones, namely low (11.928%; 354.884 km^2), moderate (76.44%; 2274.4 km^2), and high (11.267%; 345.943 km^2), in sequential sequence. These categories define the model's output in descending order of how closely it matches the actual conditions. After that, a map removal sensitivity analysis was also executed and found that geology, geomorphology, lineament density and drainage density strongly influence the prediction model for groundwater potential zone identification. The reliability of the results is established by employing a Receiver Operating Characteristic (ROC) curve for evaluation, which demonstrates a prediction accuracy of 81.3%. Authorities responsible for groundwater resource management can use this study's findings to better inform future regulatory initiatives.

Keywords Remote sensing and GIS · AHP method · ROC curve · Trans Yamuna Region, Prayagraj

Introduction

Groundwater is one of the most important and valuable parts of the natural water cycle. It is stored in the pores of soil and rock below the water table (Fitts, 2013). One third of all freshwater withdrawals around the world come from groundwater (Taylor et al., 2013). Groundwater is the only source of water for about 2.5 billion people around the world (Unesco, 2020). It is used more and more in irrigation, factories, cities, and homes in rural areas (Todd, 2005). In India, China, and some African countries, where there are a lot of people and a lot of factories, there

Swarnim · J. N. Tripathi (✉) · I. Sonker
Department of Earth & Planetary Sciences, University of Allahabad, Prayagraj 211 002, India
e-mail: jntripathi@gmail.com

S. P. Tiwari
Applied Research Center for Environment and Marine Studies, Research Institute, King Fahd University of Petroleum and Minerals, 31261 Dhahran, Saudi Arabia

is not enough water to go around. This is because the demand for water in homes, farms, and factories has grown (Das et al., 2017; Manap et al., 2013). In India as the population is growing, they need to the farmland for agriculture purposes so deforestation and overexploitation of groundwater has occurred across the country, resulting in a subsequent decline in groundwater levels (Saranya & Saravanan, 2020). India's agricultural and drinking water security have become more reliant on groundwater. According to Ministry of (Jal-Shakti, 2020) the country's total annual groundwater recharge was calculated to be 436.15 billion cubic metres (BCM). It is estimated that 393 BCM of ground water may be extracted each year, while 432 BCM is replenished each year. The total annual groundwater extraction is 249 billion cubic metres, with 221 billion cubic metres (89%) used for irrigation and 25 billion cubic metres (11%) used for domestic and industrial purposes. According to the most current survey, 61.6% of the country's groundwater reserves have been used up (CGWB, 2021). Ground water provides the source for approximately 62% of all irrigation, 85% of all water supply in rural areas, and 45% of all water supply in urban areas. As of the year 2001, India had a per capita water availability of 1816 m^3, but experts predict that this number will fall to 1140 m^3 by the year 2050 (Narendra Modi, n.d.; Sikdar, 2018).

Aquifers holding subsurface groundwater are extremely confined and spatially variable (Satpathy & Kanungo, 1976). Knowing the present reputation of groundwater potential in any place requires knowing the prospective zone of groundwater where artificial recharge techniques can be employed to increase the amount of recharge and ensure a sufficient amount of recharge (Razandi et al., 2015). As a result, it is very important to learn how to approach groundwater management and how to predict groundwater capability on the national, regional, and local level (le Page et al., 2012; Vaux, 2011). Therefore, there is a significant amount of interest among scientists in the process of generating a map of all of the potential groundwater locations (Arabameri et al., 2018; Das & Pardeshi, 2018).

Although there are various reliable geophysical and geological methods for detecting aquifer locations and groundwater levels, employing these techniques to assess groundwater resource availability is both time-consuming and financially prohibitive

(Fetter, 2001). Recently, there has been a lot of focus placed on integrating remote sensing (RS) and the geographical information system (GIS) because it is a method of exploration that is not only efficient but also very inexpensive and rapid (Arefin, 2020a, 2020b; Chowdhury et al., 2008; Gassama Jallow et al., 2020). Because satellite data is widely available and is used in mapping and topographical processes, it is easy to put together information that can be used to evaluate places with potential groundwater capability (Magesh et al., 2011; Mallick et al., 2015).

The number of parameters that determine groundwater potentiality varies with the different research studies. Many studies focused on parameters such as Geology, Geomorphology, Slope, Soil texture, Drainage density, Lineament density, Rainfall, Land use & Land cover, Topographic Wetness Index etc. (Ganapuram et al., 2009; Israil et al., 2006; Magesh et al., 2012; Mukherjee et al., 2012; Owolabi et al., 2020) using the number of methods utilizing the thematic maps, to identify possible regions for groundwater recharge such as frequency ratio, (Manap et al., 2014; Pourtaghi & Pourghasemi, 2014; Moghaddam et al., 2015; Naghibi et al., 2016; Al-Abadi et al., 2016; Guru et al., 2017), Logistic regression model techniques (Ozdemir, 2011), evidential belief function (EBF) (Park et al., 2014; Pourghasemi & Beheshtirad, 2015), certainty factor (CF) (Razandi et al., 2015), analytical hierarchy process (AHP) (Arefin, 2020a, 2020b; Kumar & Krishna, 2018; Maity et al., 2022; Moharir et al., 2023; Muralitharan & Palanivel, 2015; Murmu et al., 2019; Saranya & Saravanan, 2020) and many other mathematical and geostatistical models. The Analytical Hierarchical Process (AHP) was shown to be a method that is effective, dependable, and practicable for identifying groundwater potential zones.

The multicollinear test is very important test that is applied to the thematic layers to improve the model's ability to make accurate predictions. Other RS/ GIS-based models, have also used this method such as landslide susceptibility, assessment of land subsidence, soil erosion susceptibility (Abdulkadir et al., 2019; Blachowski, 2016; Mallick et al., 2021; Rossi et al., 2021), and other models. Map removal sensitivity analysis is a good method to know the most significant parameters in the model output (Mukherjee & Singh, 2020; Thapa et al., 2018).

Many researches have applied this technique for groundwater and aquifer vulnerability assessments, distinct from the AHP technique (Kumar et al., 2022; Oke, 2020; Sadat-Noori & Ebrahimi, 2016). Receiver operating characteristic (ROC) curve, a cross-validation method, is used by comparing the model output with the depth of water table of the observation wells. Many researchers have used this cross-validation method to identify the groundwater potential zones (Dar et al., 2021; Hasanuzzaman et al., 2022), Landslide susceptibility (Chen et al., 2018; Gorsevski et al., 2006) and also for other analysis. For this study, the ROC curve was used for validation of groundwater potential map.

The Prayagraj district is currently facing a significant issue of water scarcity, particularly in the Trans Yamuna region. This problem has arisen due to the overexploitation of groundwater resources and the geological characteristics of the dissected plateau, which hinder the infiltration of water. (Ministry of Environment Forest and Climate Change Notification, 2018). So, it is necessary to investigate the groundwater condition in the Trans Yamuna region for sustainable management. Numerous studies have identified the groundwater potential zones in the entire Prayagraj district as well as in various parts of the district (Shukla, 2014; Syed Wamiq Ali et al., 2015; Mukesh Kumar et al., 2018; Tiwari, 2018) using different methods and multiple parameters. To delineate the groundwater potential zones in this study region, remote sensing and GIS techniques were combined with the AHP method using multiple parameters, including some parameters, multicollinearity between parameters, and map removal sensitivity analysis that had never been performed in this study region.

Hence, AHP, GIS, and RS approaches were applied to combine hydrogeological, geomorphological, and climatological data in order to identify distinct groundwater potential zones in the Trans Yamuna region within the Prayagraj district. Ten groundwater recharge affected criteria such as geology, geomorphology, soil texture, lineament density, drainage density, regional slope, rainfall distribution and land-use pattern, Topographic Wetness Index and NDVI have been investigated to make groundwater potential maps for future planning, governance, use, and conservation of groundwater resources in the study area.

Materials and methods

Study area

Prayagraj is one of the oldest and most important cities in India from a religious point of view. It is located at the confluence of the Ganga, the Yamuna, and the unseen Sarasvati. All of which are considered sacred rivers. The district is made up of three primary physical divisions: the Daob, the Trans Yamuna (or Yamunapar) tract, and the Trans Ganga (or Gangapar) plain. The Daob is the smallest of these three divisions. Our focused study area is the Trans-Yamuna tract and its geographical extent is from 24°48′10″N to 25°26′20″N latitude and 81°30′10″E to 82°20′26″E longitude. The study region consists tropical climate, which is typified by lengthy, hot summers, moderately pleasant monsoons, and chilly winters. The average amount of rain in the study region is 976 mm and mean annual temperature is 25.8 °C of different seasons of a year but the amount varies from year to year. It covers a total area of 2990.957 km^2 and has a total population of 1931247 people (Census, 2011; https://www.census2011.co.in/census/district/546-allahabad.html). The study area contains four tahsils named, Bara, Karchana, Koraon and Meja. Meja is the largest Tahsil in terms of land area, but Karchana is the largest in terms of population. In the study area, the Denudational hills (exposed rock surfaces) are quite prominent, particularly in Shankargarh, Koraon, and Meja. In the Trans Yamuna region, the thickness of alluvium is up to 75 m. Data from exploratory drilling in the district shows that fractures are found in the Trans Yamuna region. In Trans-Yamuna region mainly the rivers Yamuna, Tons and Belan River flows. The Tons River tributary of the Yamuna and the Belan River flows from Kaimur Hill and joins the Tons River at Chakghat in MP. (Pandey, 2009; District Survey Report-Allahabad (In-Situ Rock), 2018; Saha & Agrawal, 2020). The study area map is shown in the (Fig. 1).

Steps for identification of groundwater potential zones

There are five main steps for groundwater potential mapping that are applied for this research, shown in (Fig. 2) as a flow chart: (1) Choosing the controlling parameters for Groundwater potential zone (2) Creation of Geospatial database systems (conditioning factors related to groundwater potential zones) (3)
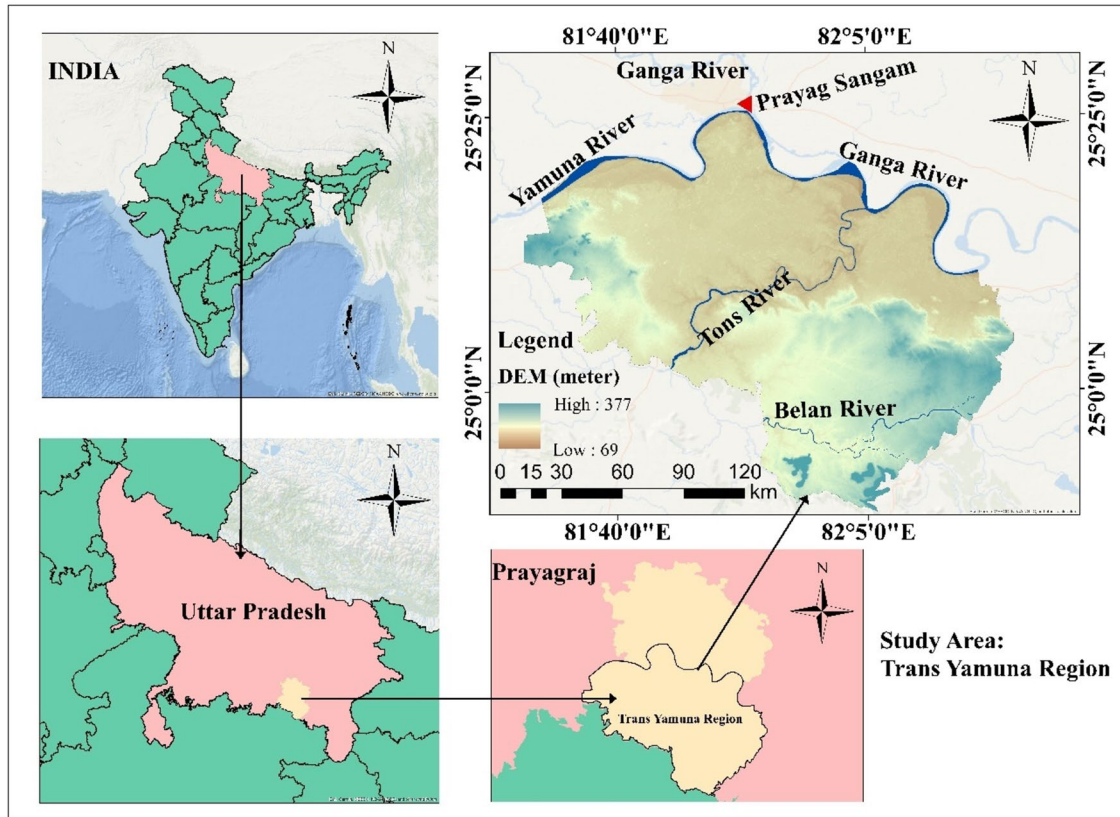
Fig. 1 Map of the study area (Trans Yamuna Region, Prayagraj, Uttar Pradesh, India)

Perform the multicollinearity test to check the collinearity among the all-selected parameters (4) Apply the AHP method, and (5) Validation of the ground water potential map.

Selection of controlling Parameters for Groundwater potential zone

The variety of conditioning parameters is determined by the availability of data in the study area that are likely to influence the groundwater potential zones. As conditioning elements, several layers, including geology, geomorphology, soil, slope angle, NDVI, LULC, topographic wetness index (TWI), precipitation, drainage density, and lineament density were selected because the presence and movement of groundwater are directly or indirectly controlled by these factors, as explained below.

Where groundwater is located and how it is distributed are heavily influenced by the geology and hydrology of a place. The amount of water, a geological formation and aquifer layer can store, give out, or take in is mostly determined by the porosity, permeability, and transmissivity of the aquifer, its interconnectivity, the types of exposed rock and subsurface rock such as sedimentary, igneous and metamorphic rocks in which sedimentary rocks are good for groundwater recharge because it has high porosity and permeability (Arefin, 2020a, 2020b), and the proximity to surface water sources (Jaiswal et al., 2003). Geomorphological features of a region help us understand how different landforms and topographic information are spread out in space, such as how groundwater moves below the surface and it help to understand lithological and structural control on groundwater potential zones (Gnanachandrasamy et al., 2018). Rainfall feeds surface water bodies and recharges groundwater through percolation. Rainfall also affects groundwater levels; however, percolation relies on strength and duration (Lakshmi et al., 2018).
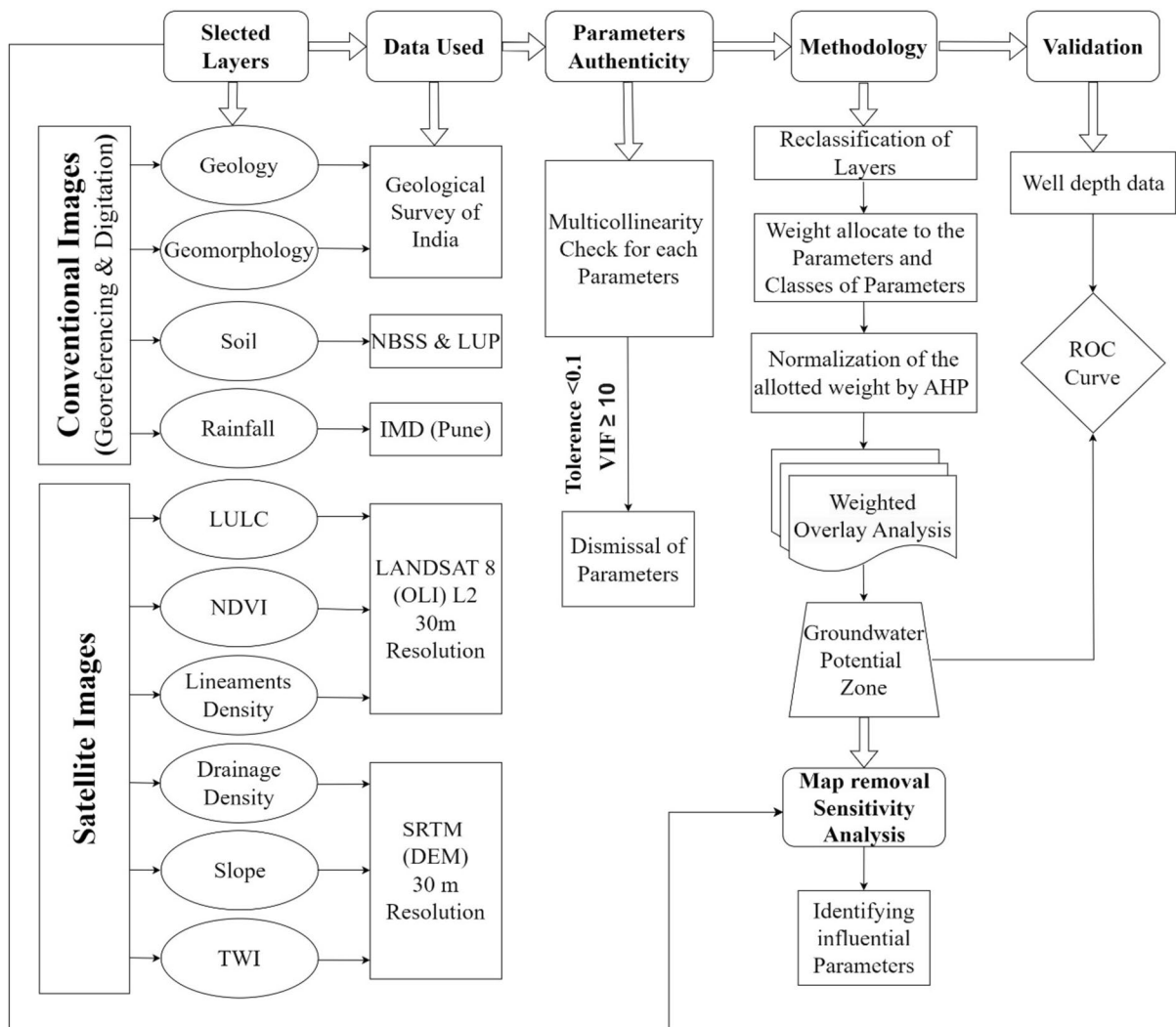
Fig. 2 Flow chart of methodology used in the present study

LULC decides the water infiltration to Groundwater recharge such as in built-up environments, where the infiltration rate is frequently lower since there are fewer permeable surfaces present. Woods and agricultural regions, on the other hand, allow more water to infiltrate because of the vegetative cover's capacity to hold onto water and encourage infiltration (Scanlon et al., 2005). Slope regulates the vertical penetration of water, particularly rainwater, and surface runoff (Dhinsa et al., 2022). Drainage density is the number of channels in a landscape and is the opposite of permeability (Mageshkumar et al., 2019). The soil is the topmost layer of the earth. It is where water seeps into the ground. The soil's ability to hold water and

how well it lets water pass through it determine the rate of infiltration (Allafta et al., 2021). The Lineaments density indicates the presence of more permeable zones which is good for groundwater recharge (Sonwane & Ullah Usmani, 2021). The topographic wetness index (TWI) is used to measure how topography impacts hydrological processes and illustrates how topography may cause groundwater seepage and it is also regarded as a secondary topographical characteristic when assessing the wetness conditions of an area (Arulbalaji et al., 2019). NDVI is a widely used as an indicator for monitoring the dynamic of vegetation at regional and global scales which signifies the groundwater potential zone (Senapati & Das, 2022).

The integration of these factors with their potential weights is calculated through weighted overlay analysis in ArcGIS software.

Geospatial database preparation

The base map of the Trans Yamuna Region was created using Survey of India toposheets (No. 63G/11, 12, 15, 16; 63H/13; 63 K/3, 4, 7, 8; 63L/1, 5) at a scale of 1:50,000. Thereafter, all toposheets is merged and study area boundary was extracted by digitizing in Arc GIS software. The satellite images of study area, SRTM DEM 30 m Resolution and LANDSAT 8 OLI/ TIRS C2 L2 Image, freely downloaded by https://earthexplorer.usgs.gov/ (Table 1). By using the SRTM DEM data the Slope, Drainage density, Topographic wetness index and Lineament density, Land use & Land cover, Normalized Differential Vegetation Index map were prepared using the LANDSAT 8 multiband data with the help of ArcGIS software of the study area. The Geology and Geomorphology map was prepared using the geological and geomorphological maps obtained from the Geological Survey of India on a scale of 1:250000 and 1:100000, respectively. The previous soil map that was created by the Indian Council of Agriculture Research's National Bureau of Soil Survey and Land Use Planning Office (NBSS and LUP) served as the basis for the generation of a new soil map at a scale of 1:50000 (ICAR). By georeferencing the maps with Georeferencing tools and digitising them with the Arc Scan tool in the ArcGIS software, these thematic layers were produced. The Indian Meteorological Department

(IMD) Pune provided the rainfall data for the years from 1990 to 2020 that was used in this study. The rainfall data was analyzed to produce a thematic layer using a geostatistical kriging interpolation method in a geographic information system. The false colour composite (FCC) image of LANDSAT data was visually interpreted with image interpretation keys along with shape, size, tone, texture, pattern, and affiliation to determine lineaments for the preparation of lineaments density maps and land use & land cover maps using the line density analysis tool and the Supervised classification tool respectively in ArcGIS software. The slope map is produced by the surface function from spatial analyst tool in the Arc GIS software using the projected Digital Elevation Model. To produce the Drainage density map, the drainage network was generated using the function of Hydrology module of the Spatial Analyst tool such as Fill, Flow direction, Flow accumulation, Stream Order, and Stream to Feature. These functions were used to generate a drainage network map, which was then used to generate the drainage density map. The raster calculator tool was used for numeric calculations to generate the drainage density map. The topographic wetness index was developed using the TOPMODEL index (Beven, 1997; Guisan et al., 1999). These all-thematic layers are geo-coded with the Universal Transverse Mercator (UTM) projection, a spherical coordinate system, and a World Geodetic System (WGS) 84, Zone 44 North. After that, each thematic layer has been changed to 30 m resolution raster format. In a GIS environment, all thematic layers are integrated using the weighted overlay method to generate one

Table 1 Information about the parameters, datatype and dataset used in the present study

Parameters	Data type	Resolution/Scale	Sources
Geology	Polygon	1: 250,000	https://www.gsi.gov.in/
Geomorphology	Polygon	1: 100,000	https://www.gsi.gov.in/
Soil	Polygon	1: 50,000	https://nbsslup.icar.gov.in/soil-resource-studiessrs/
Rainfall	Gridded	0.25 Degree	https://cdsp.imdpune.gov.in/
Land use & Land Cover	Raster	30 m, Landsat 8 (OLI)	https://earthexplorer.usgs.gov/
NDVI	Raster	30 m, Landsat 8 (OLI)	https://earthexplorer.usgs.gov/
Lineament Density	Raster	30 m, Landsat 8 (OLI)	https://earthexplorer.usgs.gov/
Drainage Density	Raster	1 arc second (30 m) SRTM (DEM)	https://earthexplorer.usgs.gov/
Slope	Raster	1 arc second (30 m) SRTM (DEM)	https://earthexplorer.usgs.gov/
TWI	Raster	1 arc second (30 m) SRTM (DEM)	https://earthexplorer.usgs.gov/
Well data	Points	—	(https://bhuvan-app1.nrsc.gov.in/gwis/gwis.php#

map of the groundwater potential zones of the study area. For validation the water level depth of well data is taken from CGWB department.

Multicollinear test

When one independent parameter has a strong association with another parameter, this is known as multicollinearity and presents a challenge in a multi regression model. This makes it difficult to evaluate the quality of the model (Mukherjee & Singh, 2020). Prior to the selection of parameters for delineating the groundwater potential zone, the multicollinearity test is an absolutely necessary step. If a given parameter exhibits a high correlation to any other parameter, this denotes that any change in the value of one parameter will cause a corresponding change in the value of the other parameter, which in turn will cause variations in the model's results. If a given parameter does not exhibit a high correlation to any other parameter, the model's results will remain consistent regardless of the value of any given parameter. This implies that non-trivially accurate predictions can be made for any input parameter given a set of other parameters (such as slope and slope aspects) (Saha, 2017).

To determine the accuracy of this validation, a linear regression analysis is performed, with one parameter serving as the dependent variable and the remaining parameters serving as the independent variables to calculate the tolerance and variance inflation factor (VIF). Tolerance and VIF values can be calculated for each parameter by repeating the preceding steps. The following equations is used to evaluate the tolerance and variance inflation factor (VIF).

$$Tolerance = 1 - R^2 \qquad (1)$$

$$VIF = \frac{1}{Tolerance} \qquad (2)$$

Equations (1, 2) are going to be used, one at a time, for the many other parameters. VIF values between 1 and 5 are generally considered acceptable, suggesting low to moderate multicollinearity and a tolerance value close to 1 suggests no or little multicollinearity. Tolerance values less than 0.2 or 0.1 indicate high multicollinearity (Al-Fugara et al., 2020). 300 random points were selected from 10 groundwater-determining theme layers for the multicollinearity test.

According to this conclusion, there is no collinearity between any of the ten factors that determine the potential of groundwater (Table 2).

Derivation of normalized weights of thematic layers and evaluation of the groundwater potential zones by AHP method

The Analytical Hierarchy Process (AHP) is the most effective for modelling the resolution of multiple criteria (Saaty & Vargas, 1980). The relative significance of each individual layer can be determined by utilising Saaty's scale, which ranges from 1 to 9 (Table 3), wherein a rating of 1 denotes identical significance among the two parameters, and a rating of 9 suggests the outrageous importance of 1 parameter contrasted with the other one (Saaty, 1990).

According to (Alesheikh & Hosseinali, 2008) following steps comprise for the Analytical Hierarchy process method.

1. Making pairwise matrix on the basis of mutual importance and did normalization.

$$Z = \begin{matrix} x_{11} & , & x_{12\cdots} & x_{n1} , \\ x_{21} & , & x_{22\cdots} & x_{n2,} \\ \vdots & \vdots & \ddots & \vdots \\ x_{n1} & , & x_{n2\cdots} & x_{nn,} \end{matrix}$$

$$Normalization(W) = \frac{1}{n} \Sigma \frac{x_{ab}}{\sum_1^n x_{ab}} \qquad (3)$$

Here a, b = 1 ,2 ……., n

Table 2 Statistics on the collinearity of the factors

Sr No	Layers	Tolerance	VIF
1	Lineaments density	0.966511	1.034649373
2	Drainage density	0.992256	1.007804438
3	Geology	0.869679	1.149849542
4	Geomorphology	0.775324	1.289783368
5	LULC	0.917056	1.090445949
6	NDVI	0.998400	1.001602564
7	Rainfall	0.826111	1.210491084
8	Slope	0.927639	1.078005560
9	Soil	0.931356	1.073703289
10	TWI	0.937999	1.066099218

Table 3 Scale preferred by Saaty for comparing two AHP parameters

Rating of significance	Definition	Explanation
1	Equal significance	Two activities behave equally to the objective
3	Weak significance of one over another	One activity has a modest advantage over another based-on experience and judgement
5	Strong significance	One activity has a strong or essential advantage over another based-on experience and judgement
7	Demonstrated significance	An activity is vigorously favoured, and its dominance is demonstrated in practice
9	Absolute significance	The evidence that favours one action over another is at the highest level of assurance
2,4,6 and 8	Intermediate number between two adjacent numbers	When compromise is essential
Reciprocals of above non zero	When activity I is compared to activity j and one of the above non-zero integers is assigned to it, then j has the reciprocal value	

For pairwise matrix construction, the values assigned to a and b according to the Table 3 are determined by the Saaty's scale.

2. The conventional eigenvalue method in the analytic hierarchy process allows for the measurement of the consistency of the author's preferences as represented in the comparison matrix and provides a way to evaluate the coherence of their judgments (Antonio Alonso & Teresa Lamata, 2006). The principal eigenvalue value (λ_{max}) was analysed using eigen vector method.

$$ZW = \begin{bmatrix} x_{11}, x_{12}...x_{1n}, \\ x_{21}, x_{22}...x_{2n}, \\ \vdots \vdots \ddots \vdots \\ x_{n1}, x_{n2}...x_{nn}, \end{bmatrix} x \begin{bmatrix} w_1 \\ w_1 \\ \vdots \\ w_j \end{bmatrix}$$

Here W designate the normalized value

$$\lambda_{max} = \frac{1}{n} \Sigma \frac{\Sigma ZW}{w_j} \tag{4}$$

Here ΣZW = Addition of Row, w_j = Each value of Normalized weight, n = Number of factors.

The groundwater potential mapping approach is based on the fact that the authors expertise determines the relative importance of each of the numerous thematic layers and their teachings. Thus, each element that impacts the quantity of groundwater in a particular region is assigned the appropriate rank and weight according to Table 4.

3. Consistency of the model

o   3(a). The consistency index indicates the degree to which the matrix is inconsistent and the degree to which our matrix is inconsistent in comparison to a consistent matrix. In the case of a fully consistent matrix, the average of the remaining eigenvalues is zero, resulting in a Consistency Index (CI) value of 0 (Pant et al., 2022)

Consistency index of Z express by the formula of (Saaty, 2008)

$$C = \frac{\lambda_{max} - n}{n - 1} \tag{5}$$

Here, λ_{max} = biggest eigenvalue of the matrix and may be without problems decided from the mentioned matrix, and n = number of groundwater conditioning aspects.

o   3(b). The consistency ratio measures consistency index relative to a random index value. The random index represents the average inconsistency estimated in a random comparison matrix of the same size. (Saaty, 1980). Consistency ratio (CR) express by the formula, (Saaty & Vargas, 1980)

$$CR = \frac{(Consistency\ index)}{(Random\ consistency\ index)} \tag{6}$$

Table 4 Weight assignment to different parameters and reason behind that

Parameters	Weight-assigning procedure	Logic	References
Geomorphology (GM)	Highest rank assigned to the water bodies and reservoir and lowest rank assigned to the lower dissected plateau	Denudational hills function as runoff zones due to their hard, compact nature, little infiltration, and minimal groundwater potential	Verma & Patel, 2021
Geology (GL)	Highest rank given to the Alluvium and lowest rank given to the kaimur group	Kaimur group mostly consists Quartzite, has the low porosity and permeability and Alluvium has high porosity and permeability compare to the Quartzite	Kumar & Krishna, 2018
Lineament Density (LD)	Higher rank assigned to the higher lineament density	Higher lineament density allows the water infiltration more	Kindie et al., 2019
Drainage Density (DD)	Higher rank is given to the drainages with the lower density	A low GWPZ corresponds to a high drainage density and vice versa	Pinto et al., 2017
LULC	Higher rank given to the dense vegetation and water body and lower rank is assigned to the settlement area	Due to the prevalence of impermeable surfaces in settlement area, infiltration rates and capacities are low	Arulbalaji et al., 2019
Soil (S)	Higher rank given to the loam soil and lower rank is assigned to the clayey loam soil	Infiltration rate of water in clayey loam soil is very low and comparatively high in the loamy soil	Berhanu et al., 2013; Allafta et al., 2021
NDVI	Higher rank is given to the higher and lowest value normalized differential vegetation index	Higher value denotes the dense vegetation and lower value denote the water bodies	Senapati & Das, 2022
Slope (SL)	Higher rank assigned to the flat and lowest slope area	Due to the increased velocity of the water on a steep slope, runoff happens quickly	Das et al., 2017
TWI	Higher rank is given to the higher value of TWI	The TWI shows where the wetness is located across the globe. It regulates the gravitational pull of water and its tendency to accumulate on the slope	Melese & Belay, 2022; Mukherjee & Singh, 2020
Rainfall (Rf)	Higher rank is given to the maximum rainfall value	There is a strong positive association between rainfall and groundwater, according to multiple studies	Doke et al., 2021; Maity et al., 2022

The random consistency index is given according to the Table 5. If the CR occur < 0.1, then the given weight for the matrix is reliable if the CR occur > 0.1 then need to check again the assigned weight for the matrix (Saaty, 1990; Sonwane & Ullah Usmani, 2021).

In this work, a lot of existing literature (Agarwal et al., 2013; Bera et al., 2020; Castillo et al., 2022; Ifediegwu, 2022; Kaliraj et al., 2014; Kumar & Krishna, 2018; Mahato et al., 2021; Narayanamurthi & Ramasamy, 2022; Patra et al., 2018; Pinto et al., 2017; Rajasekhar et al., 2019; Rajesh et al., 2021) was carefully looked at before preparing the pairwise matrix and analysis of the consistency Tables 6 and 7. This was done so that we could get a good idea of how variables rank in different environments and in different places.

Groundwater potential index is a non-dimensional number that can be used to predict the groundwater potential zones in a certain region (Zhang et al., 2021). Arc GIS weighted overlay function was used for this evaluation. The normalized weight of the aspect was multiplied by the weights of classes of every aspect after that summed the multiplication of all of the attributes and obtained the groundwater potential zone (GPZ) which can be evaluated according to (Muralitharan & Palanivel, 2015; Biju et al., 2018; Doke et al., 2021; Maity et al., 2022) using following equation.

$$GPZ = \text{Total of the aspects normalised weight}(W)$$
$$\times \text{weight of each aspects class}(I) \dots \tag{7}$$

Validation of the map revealing the groundwater potential zone

Several analyses, making use of the obtainable well depth data, have validated the groundwater potential zone (Dar et al., 2021; Naghibi et al., 2016). The Receiver Operating Characteristic ROC and Area Under Curve (AUC) have been used to evaluate groundwater potential maps for accuracy in several research projects (Boughariou et al., 2021; Castillo et al., 2022). The ROC curve shows how the false-negative (X-axis) and false-positive (Y-axis) rates balance out for each possible cut-off number. This compromise can be seen as a decrease in the false-negative rate while an increase in the false-positive rate. In ROC curve analysis, the capacity of a prediction system to properly predict previously defined "occurrences" is measured by an indicator called the area under the curve (AUC) (Gorsevski et al., 2006; Ozdemir, 2011; Kim et al., 2019). According to the AUC curve range varies from 0.5 to 1 in which "0.5–0.6," "0.6–0.8," "0.8–0.9," and "0.9–1.0" which correspond to "poor," "average," "good," "very good," and "excellent" respectively (Mohammady et al., 2012; Pourtaghi & Pourghasemi, 2014; Razandi et al., 2015).

Result and discussion

In this study there are 10 major responsible factors such as geology, geomorphology, lineaments density, slope, topgraphic wetness index, drainage density, rainfall, soil and land cover and land use, NDVI used for their correlation to identify the groundwater potential zone.

Geology (GL)

The study area comprised Vindhyan supergroup and Quaternary sediment rock of the age from Proterozoic to Recent Quaternary sediments. There are two types of alluvium found in the Quaternary sediments: older alluvium and newer alluvium. The Vindhyan supergroup is further subdivided, with the Kaimur rock group consisting of Quartzites and covering about 13.2% (i.e., 394.651 km^2) of the land area, and the Rewa rock group consisting of Shale and Sandstone covering about 4.29% (i.e., 128.455 km^2) of the land area. The Laterite Mantle lies beneath the crust of quartzite rock.

Table 5 Satty's Random inconsistency (RI) for various n criteria

n	1	2	3	4	5	6	7	8	9	10
RI	0	0	0.58	0.89	1.12	1.24	1.32	1.41	1.45	1.49

Table 6 Constructing the pairwise comparisons matrix based on Mukherjee & Singh (2020) and Arulbalaji et al. (2019) and checking the thematic layers' consistency, *GM* geomorphology, *GL* geology, *LD* lineament density, *DD* drainage density, *LULC* land use & land cover, *S* soil type, *NDVI* Normalized Differential Vegetation Index, *SL* slope, *TWI* Topographic Wetness Index, *Rf* rainfall

	Assigned weight	GM	GL	LD	DD	LULC	S	NDVI	SL	TWI	Rf	Normalized Weight	Normalized λ	λ_max	CI	CR
GM	9	9/9	9/8	9/8	9/7	9/7	9/6	9/5	9/4	9/3	9/2	0.17	10.20	10.10	(10.10−10)/(10−1)=0.01	0.01
GL	8	8/9	8/8	8/8	8/7	8/7	8/6	8/5	8/4	8/3	8/2	0.12	9.71			
LD	8	8/9	8/8	8/8	8/7	8/7	8/6	8/5	8/4	8/3	8/2	0.10	9.17			
DD	7	7/9	7/8	7/8	7/7	7/7	7/6	7/5	7/4	7/3	7/2	0.12	9.92			
LULC	7	7/9	7/8	7/8	7/7	7/7	7/6	7/5	7/4	7/3	7/2	0.10	9.92			
S	6	6/9	6/8	6/8	6/7	6/7	6/6	6/5	6/4	6/3	6/2	0.09	10.20			
NDVI	5	5/9	5/8	5/8	5/7	5/7	5/6	5/5	5/4	5/3	5/2	0.09	10.63			
SL	4	4/9	4/8	4/8	4/7	4/7	4/6	4/5	4/4	4/3	4/2	0.07	9.71			
TWI	3	3/9	3/8	3/8	3/7	3/7	3/6	¾	3/4	3/3	3/2	0.07	10.20			
Rf	2	2/9	2/8	2/8	2/7	2/7	2/6	2/5	2/4	2/3	2/2	0.06	11.33			
Total		6.56	7.38	7.38	8.43	8.43	9.83	11.8	14.75	19.67	29.5					

Older alluvium includes both the Banda and Varanasi alluvium; however, the Banda alluvium accounts for the greater proportion of the total area approximately 1914.61 km² (i.e., 64.01%) and the Varanasi Alluvium occupies the area about 374.849 km² (i.e., 12.53%). Over the Kaimur and Rewa Group, river material has accumulated to form the Banda Alluvium. The lower part is composed of yellowish to brown silt–clay, while the higher part is composed of coarse to fine sand and reddish-brown silt in abundance. The Newer Alluvium, which comprises Terraces, and channel Alluvium consist the area about 73.31 km² (i.e., 2.45%) and 25.35km² (i.e., 0.84%), respectively. Terraces Alluvium and channel Alluvium is manly composed of medium- to fine-grained sand and fine- to medium- grained sand with thin layers of silt and clay (Fig. 3). Highest weight assigned to Quaternary sediment with high permeability and poor holding capacity, and lower weight assigned to Vindhyan supergroup in which Rewa group is assigned by bigger weight than kaimur group because Rewa group contains more permeable Sandstone than kaimur group Quartzite (Kumar Dinkar et al., 2019; Singh & Srivastava, 2011).

Geomorphology (GM)

Geomorphology is the study of the structure and evolution of landforms, which is crucial to understanding the availability and distribution of underground water (Biswas et al., 2012; Waikar & Nilawar, 2014). The area under study consists of seven different geomorphological formations according to their origin. The pediplain–pediment complex, low and medium dissected structural lower plateau, and the younger and older alluvium plain are all the results of denudational processes, while others are the result of depositional processes, such as the younger and older alluvium plain. Most of the denudational hills are covered with vegetation and have a low rise. The study region is mostly covered by pediplain–pediment complex which comprises the 55.85% (i.e., 1671.7km²) of the total area. Second most covering part of the area is Alluvial plain which covers almost 27.7% (i.e., 829.33 km²) of the total area. The denudational hills were found at two locations which is situated in south east region in the study area. The low dissected plateau comprises the 4% (i.e., 120.7km²) of the total about and moderately dissected plateau cover the area 8.7% (i.e., 258.9 km²) of the whole area. There are

Table 7 The assigned and normalized weight of different classes for different Parameters for groundwater potential zoning

Parameters	Class	Assigned Weight	Normalized weight	λ	λ_{max}	CI	CR
Geomorphology (GM)	Moderately Dissected Plateau	2	0.061	7	7	(7–7)/ (7–1)=0	0
	Low Dissected Plateau	1	0.030	7			
	Alluvial Plain	6	0.182	7			
	Flood Plain	6	0.182	7			
	Waterbody—River	7	0.212	7			
	Dam and Reservoir	7	0.212	7			
	Pediment Pediplain Complex	4	0.121	7			
Geology (GL)	Rewa Group	2	0.065	7	7	(7–7)/ (7–1)=0	0
	Kaimur	1	0.032	7			
	River	7	0.226	7			
	Banda Alluvium	4	0.129	7			
	Varanasi Alluvium	5	0.161	7			
	Terrace Alluvium	6	0.194	7			
	Channel Alluvium	6	0.194	7			
Lineaments density (LD)	0–01—0.2	1	0.350	5	5	(5–5)/ (5–1)=0	0
	–.2—0.38	3	0.250	5			
	0–38—0.64	4	0.200	5			
	0–64—1.02	5	0.150	5			
	1–02—1.74	7	0.050	5			
Drainage Density (DD)	0–34—0.83	7	0.050	5	5	(5–5)/ (5–1)=0	0
	0–83—1.03	5	0.150	5			
	1–03—1.22	4	0.200	5			
	1–22—1.47	3	0.250	5			
	1–47—2.44	1	0.350	5			
LULC	Agriculture	4	0.154	6	6	(6–6)/ (6–1)=0	0
	Sparse vegetation	5	0.192	6			
	settlement area	1	0.038	6			
	Dense vegetation	7	0.269	6			
	Ponds	7	0.269	6			
	Bare land	2	0.077	6			
Soil (S)	Silty Loam Soil	3	0.228	3	3	(3–3)/ (3–1)=0	0
	Loamy Soil	6	0.456	3			
	Clayey Loam Soil	1	0.076	3			
NDVI	-0–09—0.07	1	0.350	5	5	(5–5)/ (5–1)=0	0
	0–07—0.12	3	0.250	5			
	0–12—0.15	4	0.200	5			
	0–15—0.19	5	0.150	5			
	0–19—0.41	7	0.050	5			
Slope (SL)	0—1.18	7	0.050	5	5	(5–5)/ (5–1)=0	0
	1–18—3.55	5	0.150	5			
	3–55—8.74	4	0.200	5			
	8–74—18.2	3	0.250	5			
	1–.2—60.27	1	0.350	5			

Table 7 (continued)

Parameters	Class	Assigned Weight	Normalized weight	λ	λ$_{max}$	CI	CR
TWI	2–83—7.51	1	0.350	5	5	(5–5)/ (5–1)=0	0
	7–51—9.2	3	0.250	5			
	–.2—11.35	4	0.200	5			
	11–35—14.35	5	0.150	5			
	14–35—22.42	7	0.050	5			
Rainfall (Rf)	713–56—770.75	1	0.350	5	5	(5–5)/ (5–1)=0	0
	770–76—810.19	3	0.250	5			
	81–.2—851.61	4	0.200	5			
	851–62—895.98	5	0.150	5			
	895–99—965	7	0.050	5			

Fig. 3 Geological map of the Trans Yamuna Region, Prayagraj
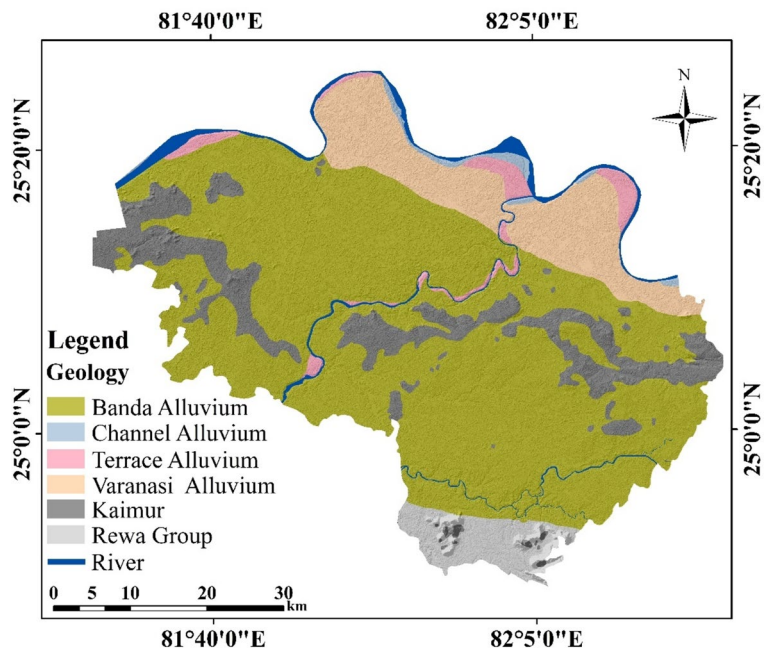
some natural and artificial reservoirs and ponds in the study area which covers the area about 0.22% (i.e., 6.8 km^2) of the whole area. Dams and check dams were built to make these lakes and ponds. Most of the time, croplands, lowlands, and hills with or without plants are all linked to each other (Fig. 4).

Land use/land cover (LULC)

On the surface of the earth, land usage refers to things that people control, like urban areas, vegetation cover, and industries. On the other hand, land cover includes elements such as water bodies, barren soil, mountains, forests, and exposed rocks. Both land cover and land use are considered landforms (Murthy & Mamo, 2009). It demonstrates the importance of groundwater supply and development in any given region (Scanlon et al., 2005). Due to the lack of permeable surfaces, water infiltration abilities are often diminished in urban and arid environments with minimal vegetation cover. Both land that is covered in vegetation and land that is used for agriculture have

Fig. 4 Geomorphology map of the Trans Yamuna Region, Prayagraj
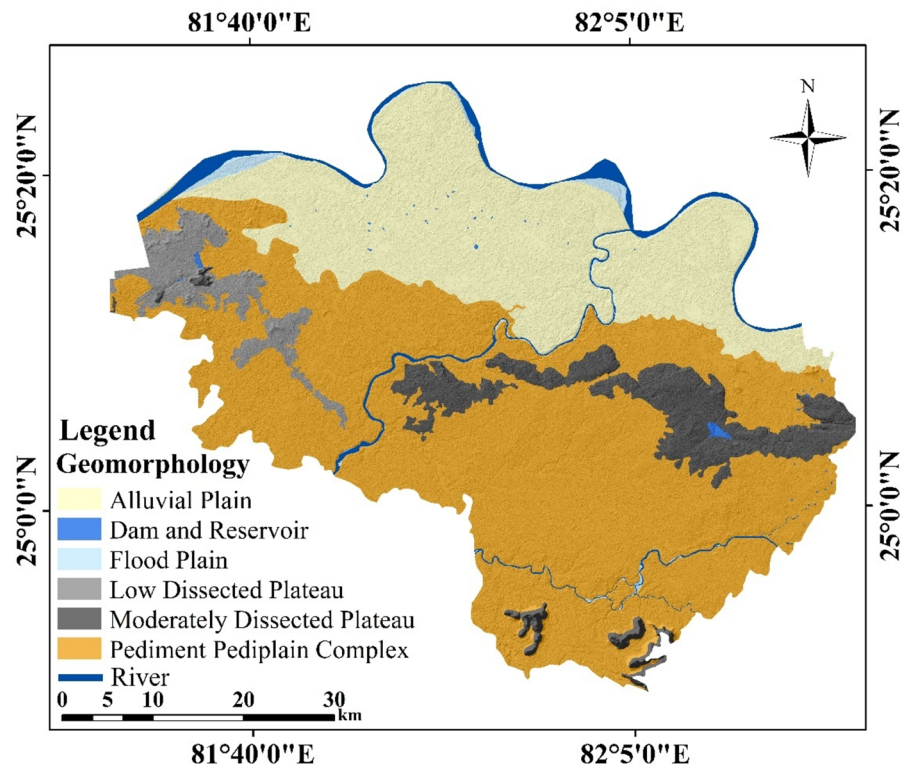
a significant potential for water infiltration, although agriculture infiltrates water to a lesser degree than does land covered in vegetation. Bodies of water are ideal for recharging aquifers. For this study the LULC map was prepared with the help of supervised classification and classified into six classes. The majority of the studied area (1901 km^2; 63.59%) is devoted to agricultural use, followed by scant vegetation (528.28 km^2; 17.67%), bare ground (293.92 km^2; 9.83%), urbanized land (169.83 km^2; 5.68%), water bodies (63.29 km^2; 2.11%), and dense vegetation (33.03 km^2; 1.10%) (Fig. 5). This map was classified with help of Supervised classification method in ERDAS IMAGINE 2014. For the accuracy assessment of the LULC the kappa statistics is important method (Islami et al., 2022; Kafi et al., 2014). For this classified map kappa statistics is used and the accuracy for this map is 83.5%. For kappa statistics the 110 random points were generated and a matrix Table 8 was created for further calculations. The output of these calculations was given in the Table 9.

Soil (S)

It is of the utmost significance for the soil to play a part in the processes of percolation and infiltration as it pertains to the recharging of groundwater (Jasrotia et al., 2016). Varying varieties of soil allow water to move laterally or vertically at different rates due to changes in the soil's distinguishing properties, such as size, texture, arrangement, and the pore spaces in between the soil grain. These variations are due to the varying degrees of permeability of the soil to the movement of water. These variations can be attributed to the soil's ability to accommodate water movement (Kumar et al., 2022). On the basis of textural analysis of soil, the Trans Yamuna region is covered by mainly Clayey loamy, Loamy, silty loamy. Type of soil (Fig. 6). Mostly part of the region is dominated by the Loamy soil (1965.1 km^2; 65.70%) area followed by silty Loamy soil (555.32 km^2; 18.57%) and Clayey loamy soil (470.54 km^2; 15.73%).

Fig. 5 Land use and land cover map of Trans Yamuna Region, Prayagraj
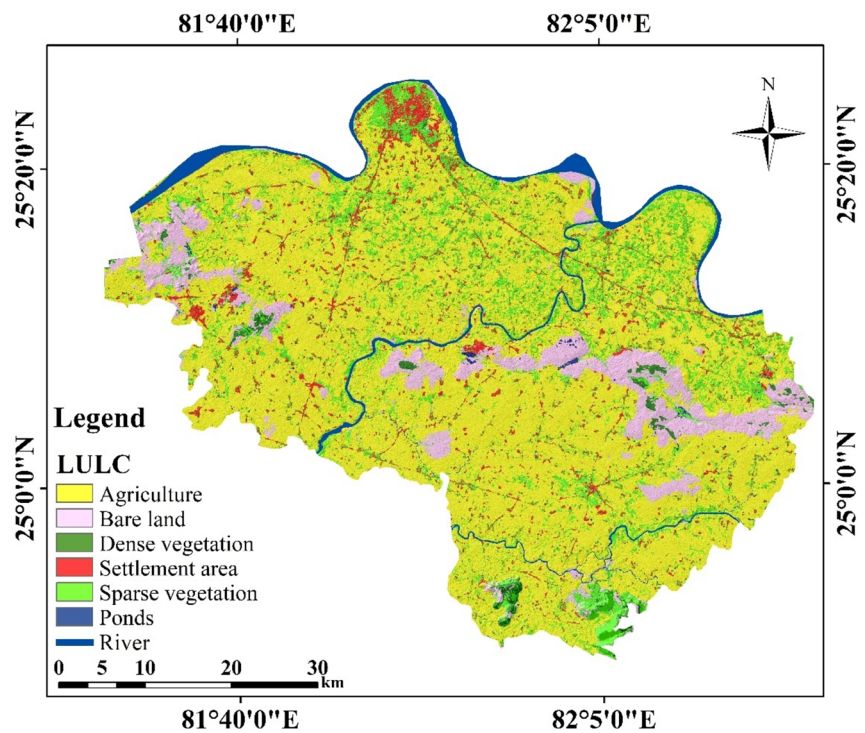
Table 8 Table used for evaluating the accuracy of LULC

	Sparse vegetation	Bare land	Dense vegetation	Agriculture	Settlement area	Water bodies	Total User
Sparse vegetation	17	0	0	6	0	1	**24**
Water bodies	0	13	0	0	0	0	**13**
Dense vegetation	0	0	11	0	0	0	**11**
Agriculture	1	0	0	16	0	0	**17**
Settlement area	0	0	0	1	22	0	**23**
Bare land	2	0	0	4	0	16	**22**
Total Producer	**20**	**13**	**11**	**27**	**22**	**17**	

Total sample = 110

Total correct sample = 95

To get the output, the following equations was used

$$\text{Overall accuracy} = \frac{\text{Total no of correctly classified pixels}}{\text{Total no of Reference pixels}} \times 100$$

$$\text{Users accuracy} = \frac{\text{Total no of correctly classified pixels in each parameter}}{\text{Total no of Reference pixels (The Row Total)}} \times 100$$

$$\text{Producer accuracy} = \frac{\text{Total no of correctly classified pixels in each parameter}}{\text{Total no of Reference pixels (The column Total)}} \times 100$$

$$\text{Kappa coefficient} = \frac{(TS \times TCS) - \Sigma(Column\ total \times Row\ total)}{Ts^2 - \Sigma(Column\ total \times Row\ total)} \times 100$$

Rainfall

Rainfall is one of the main things that affects groundwater recharge. Infiltration and percolation, which impact groundwater recharge, are affected by the intensity and duration of rainfall. Greater amounts of precipitation that fall in a shorter amount of time suggest less percolation of water and higher rates of surface water flow, and vice

Table 9 Table containing values obtained after evalution for checking the accuracy of LULC

	Producer accuracy (%)	User accuracy (%)	Overall accuracy (%)	Kappa coefficient (%)
Sparse vegetation	85	70.83333	86.36	83.5
Water bodies	100	100		
Dense vegetation	100	100		
Agriculture	59.25926	94.11765		
Settlement area	100	95.65217		
Bare land	94.11765	72.72727		

Fig. 6 Soil texture map of Trans Yamuna Region, Prayagraj
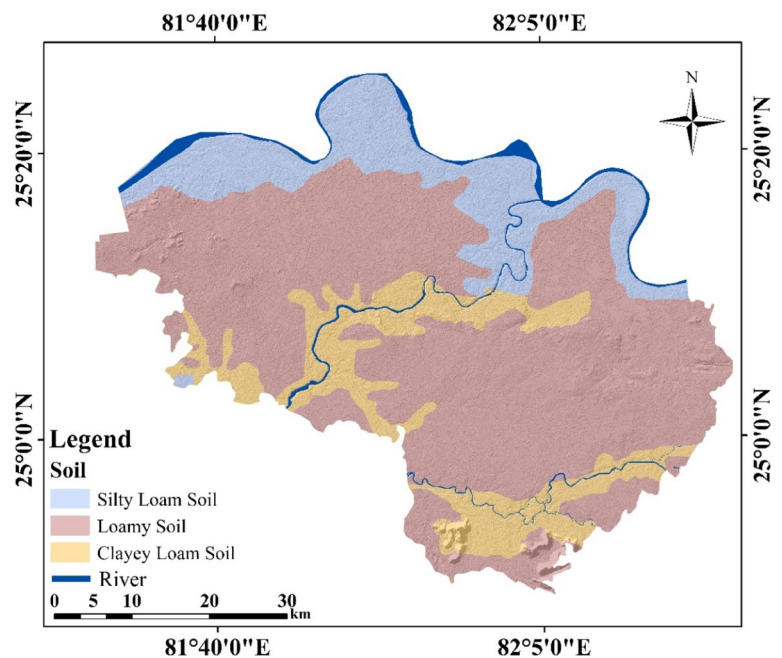
versa (Kabeto et al., 2022). The data from the year 1990 to 2020 is taken for generation the rainfall map. For this study, the rainfall map is classified into five classes such as 714–764 mm, 764–814 mm, 814–864 mm, 864–915 mm, and 915–965 mm rainfall. Rainfall map (Fig. 7) shows that very high to high rainfall occurs of south-east and very low precipitation occur in the north-west of the study area. By the (Fig. 8) it can be understood that the rainfall is minutely decreasing over the years in the Trans Yamuna Region.

Drainage density (DD)

The most important thing about hydrology is drainage density. Drainage pattern and density are caused by both surface and sub-surface features, such as the type of vegetation, structural features (Lineaments), and lithology of an area (Biju et al., 2018). Drainage density is calculated by dividing the total length of all stream segments by the area of the study area (Manap et al., 2014). It is based on following formula.

$$DD = \frac{\text{Stream Length(L)}}{\text{Basin Area(A)}}$$

The area with a very high drainage density shows that the infiltration rate is low compared to the surface runoff, and vice versa. This depends on the permeability, which in turn depends on the structurally controlled rock type of the surface and subsurface geology (Edet et al., 1998). It is clear that if the Drainage density is high,

Fig. 7 Rainfall map of Trans Yamuna Region, Prayagraj
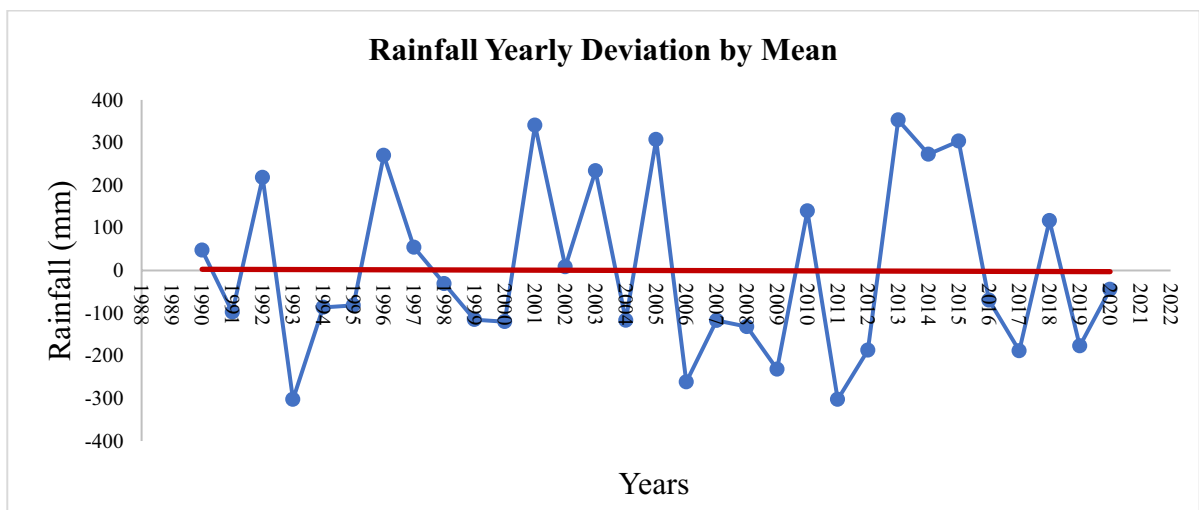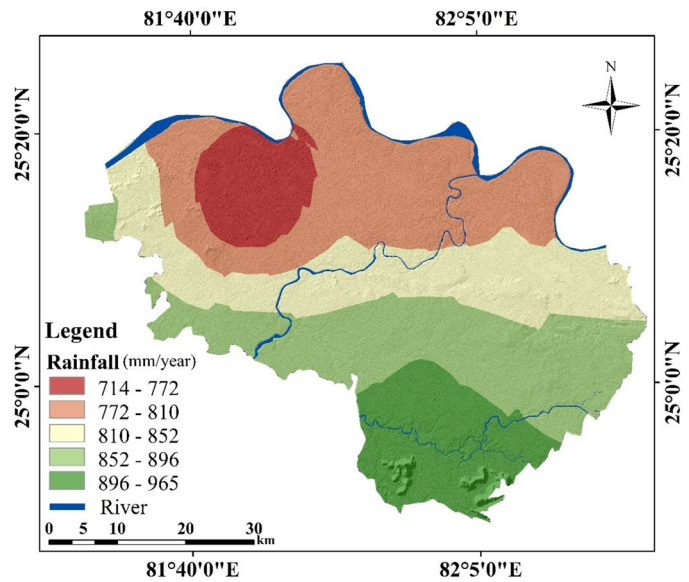
**Fig. 8** Trend of Rainfall Yearly Deviation by Mean from the year 1990 to 2020

the recharge rate will be low, and vice versa. The map of the drainage density is classified into the 5 classes such as 1.48–2.44, 1.23–1.48, 1.04–1.23, 0.84–1.04, and 0.34–0.84 km/km^2, on the basis of Drainage density value as shown in the (Fig. 9).

Lineament density (Ld)

The lineament density has a significant effect on groundwater recharge (Rejith et al., 2019; Sarmah &

Das, 2018). Joints, faults, and other surface discontinuities are reflected in the surface's lineaments, which are linear features visible from above (Han et al., 2018). Groundwater recharge in hard rock areas is done by the lineaments. High lineament density shows that the land is porous and permeable, which means that there is a lot of groundwater potential there and vice versa (Tolche, 2021). Lineament density (Ld) is defined as the total length of segmented liniments divided by the considered area (Yeh et al., 2016).

Fig. 9 Drainage density map of Trans Yamuna Region, Prayagraj
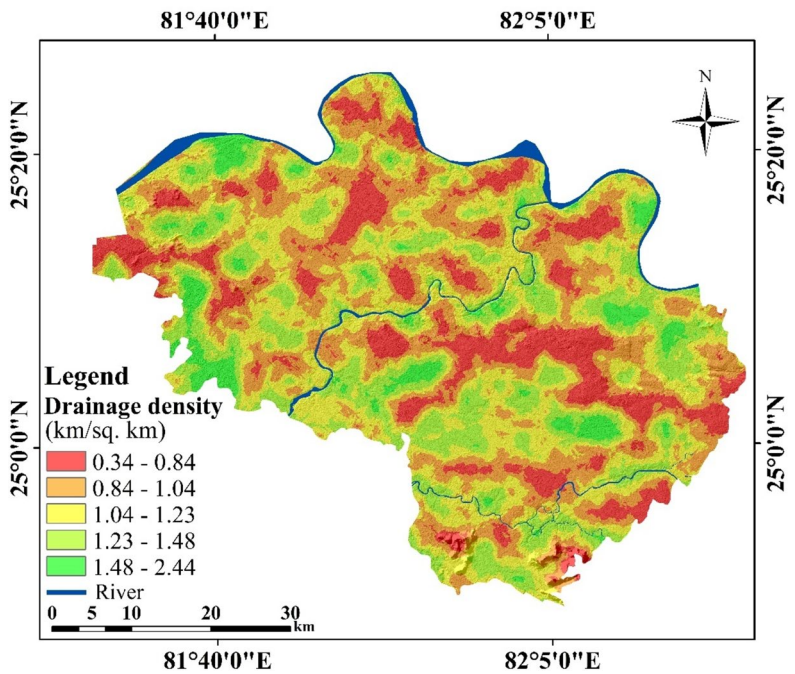
$$\text{Ld} = \frac{\sum_{i=1}^{i=n} L_i}{A}$$

$\sum_{i=1}^{i=n} L_i$ = Length of the segmented Lineaments.
A = Total Area

The study area has undulating surface and contains exposed rock of Kaimur group this Kaimur group consists mainly sandstone. So, there are many fractures and joints present in this region which liable to recharge the groundwater. In this region the lineaments are oriented in the NE—SW direction which is shown by the (Fig. 10). This map is classified into the 5 classes such as 1.03–1.74, 0.65–1.03, 0.39–0.65, 0.21–0.39, and 0.01–0.21 (very low) km/km² as shown in the (Fig. 11).

Normalized Differential Vegetation Index (NDVI)

NDVI is one of the most important parameters to delineate the groundwater potential zone. (Pande et al., 2021; Sar et al., 2015). NDVI provides a rough estimate of the amount of vegetation present
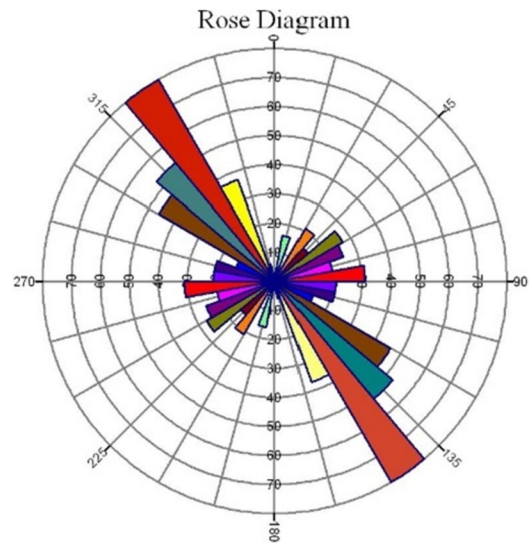
Fig. 10 Orientation of the lineaments

and the groundwater potential zones over the area (Parizi et al., 2020).

NDVI was estimated as the following formula

$$\text{NDVI} = \frac{NIR - RED}{NIR + RED}$$

Fig. 11 Lineament density map of Trans Yamuna Region, Prayagraj
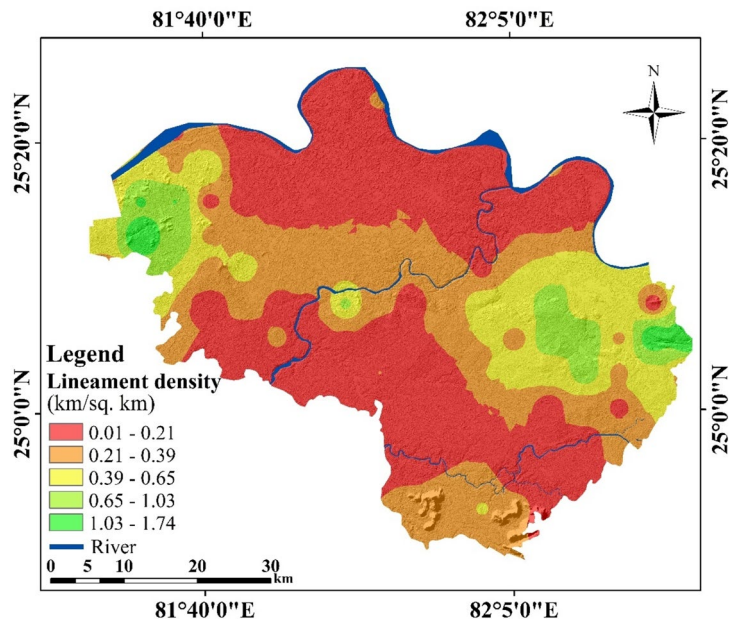
NDVI values range from -1 to +1, with values closer to 0 indicating less vegetation, such as barren land and the dark surface of bodies of water and values closer to +1 indicating more dense vegetation (Hasanuzzaman et al., 2022). In the study region, the NDVI values vary from -0.09 to 0.41 and classified into the five classes such as -0.09–0.08, 0.08–0.13, 0.13–0.16, 0.16–0.2 and 0.2–0.41, which indicate the area has moderate vegetation conditions (Fig. 12).

Slope (SL)

Slope of any area is very essential criteria to identify the groundwater potential zone (Doke et al., 2021) which is effect directly to Surface runoff, infiltration, and percolation. High slope locations do not permit groundwater recharge and increase the slope's erosion rate due to increased surface runoff, whereas gentle slope areas are suitable for groundwater recharge (Das et al., 2017). This study area has high slope area that is very less compare to the flat area and the slope map is classified into the five classes such as 0–2, 2–5, 5–9, 9–18, and 18–60 as seen in the (Fig. 13). In the study region the Kaimur rocks have high slope compared to the Alluvium. In Alluvium region soil allows the water to be infiltrate and percolate.

Topographic Wetness Index (TWI)

The TWI is a good factor for assessing the groundwater recharge. (Melese & Belay, 2022) TWI is developed in order to gain an understanding of the ways in which the structure of the terrain influences the dispersal of water and the location of areas where water accumulates. Flow direction, flow accumulation, and slope are used in mathematical formulas to figure out TWI. The higher value of the TWI designates the high ponding of water indicates the slope is gentle and helps the groundwater to be recharged (Ballerine, 2017).

TWI is calculated using the following mathematical formula,

$$I = ln\frac{\alpha}{tan\beta}$$

where α is the area attributable to the upslope and β is the topographic gradient.

In the study region the TWI is classified into the five classes such as 2.83–7.52, 7.52–9.2, 9.2–11.35, 11.35–14.35, and 14.35–22.42, as shown in the (Fig. 14).

Groundwater potential zone map of Trans Yamuna Region

Consistency ratios were determined for each factor Table 6 and the classes of each factor layer Table 7

Fig. 12 Normalized Differential Vegetation Index map of Trans Yamuna Region, Prayagraj
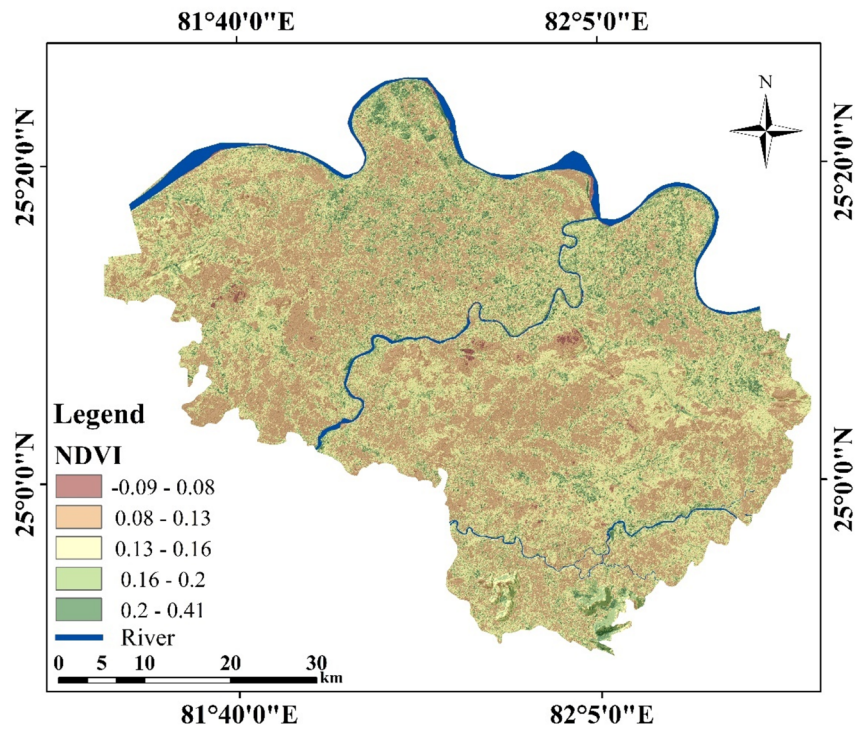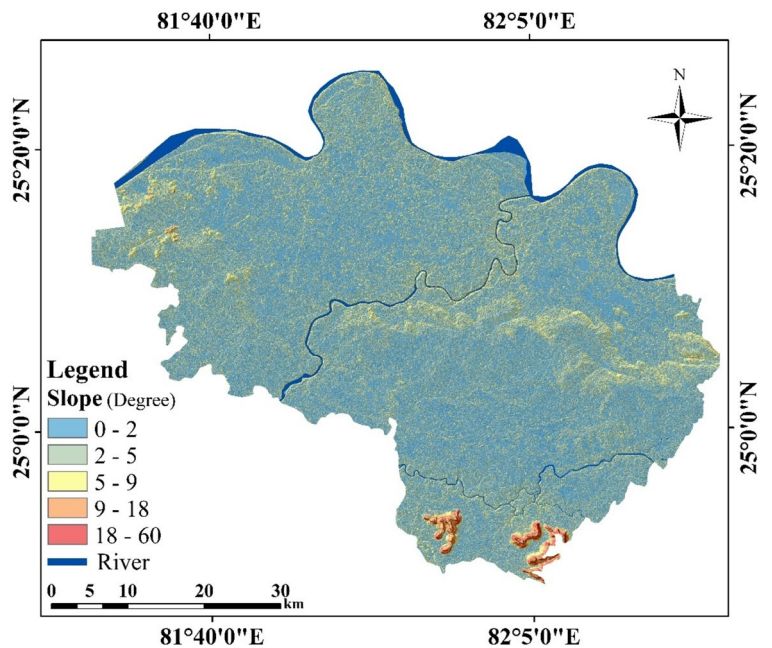

Fig. 13 Slope map of Trans Yamuna Region, Prayagraj

and the values showed that this study's judgement matrices were valid (<0.10) and had good consistency. With the help of ArcGIS, we integrated 10 thematic layers using weighted overlay in a GIS environment to produce a map of the groundwater potential zone. Linear combination equations were used to combine all 10 of the thematic layers by multiplying the weights of each theme by the weights of

Fig. 14 Topographic Wetness Index map of Trans Yamuna Region, Prayagraj
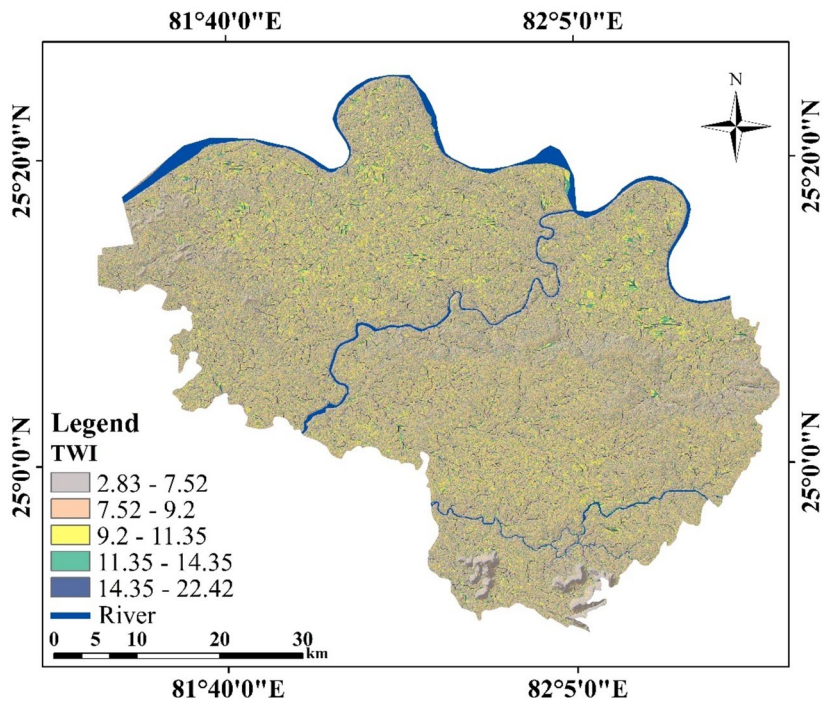
their corresponding classes to get the groundwater potential zone map using the Eq. 7 (Fig. 15). The estimated Groundwater Potential Zones of the Trans-Yamuna region were categorized into three separate classes such as low (11.928%; 354.884 km^2), Moderate (76.44%; 2274.4 km^2), High (11.267%; 345.943 km^2).

In the study region, all thematic layers influence the Groundwater Potential Zones differently. For High Groundwater Potential Zone, the Geomorphological classes, Alluvial Plain and Pediment Pediplain complex shows high impact (Fig. 16(a)) because both have relatively high porosity and permeability than other geomorphological classes in Trans-Yamuna region. The Geological classes, Banda Alluvium and Varanasi Alluvium performs good (Fig. 16(b)) because Alluvium is very high porous and permeable than other classes in the study region. The Lineament density classes such as low to moderate effect more to High Groundwater Potential Zones (Fig. 16(c)) because these classes cover most of study area than the higher lineament density classes which cover limited study area and it may drain the infiltrated water into drainages by which the percolation rate become lesser than the surface water run-off. The Drainage density classes, (0.34–0.84 km/km^2) to (1.23–1.48 km/km^2)

depict high efficacy than remaining very high drainage density class (Fig. 16(d)) because low to moderate drainage density show less surface water run-off. The LULC classes, Agriculture, Sparse vegetation and Ponds shows high influence (Fig. 16(e)) because these classes allow water to percolate beneath the earth surface and these classes cover large area of the study region than other classes. The Loamy soil, one of class of soil play a good role for High Groundwater Potential Zone (Fig. 16(f)) because this class has capability to allow surface water to percolate. The all NDVI classes depicts good condition for High Groundwater Potential Zone in the study area (Fig. 16(g)) The (0–2) degree slope, the lowest class of Slope parameter behaves good for High Groundwater Potential Zone in the Trans – Yamuna region than other high degree slope classes (Fig. 16(h)) because it restricts the surface water run-off. The class of TWI (2.83–7.52) to (11.35–14.35) has high impact on High Groundwater Potential Zone (Fig. 16(i)) because these classes responsible for groundwater recharge and cover the high study region than remaining high TWI class which contain less influence. The (772–810 mm) to (852–896 mm) classes of Rainfall depict good efficacy on High Groundwater Potential Zone than most of high rainfall class (Fig. 16(j)) because topography of study
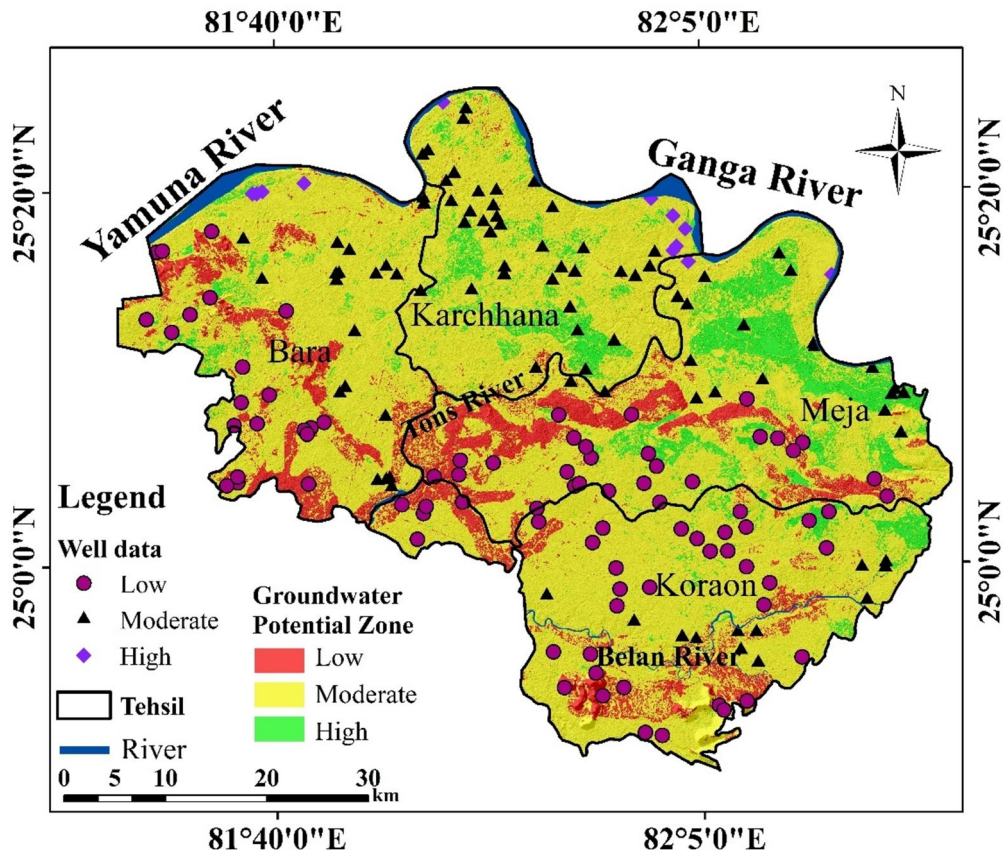
Fig. 15 Groundwater Potential Zones Map of Trans Yamuna Region

region lesser the influence of high rainfall and trigger the surface water run-off.

For Moderate Groundwater Potential Zone, the Geomorphological classes such as Pediment pediplain complex, Alluvium plain depict high influence while for Low Groundwater Potential Zone, moderately dissected plateau has high influence (Fig. 16(a)) because it has low porosity and permeability relative to Pediment pediplain complex and Alluvium plain. The Geological classes, Banda alluvium and Kaimur shows high impact on Moderate and Low Groundwater Potential Zone respectively (Fig. 16(b)) because Kaimur contains Quartzite mostly which is low porous and permeable relative to Banda alluvium. The lower to moderate classes of Lineament density show higher efficacy on Moderate as well as on Low Groundwater Potential Zone (Fig. 16(c)) because these classes cover large area of study region and High lineament density is less in the study area so it is not comparatively more effective to recharge the groundwater than other

classes. The Drainage density classes, (1.04–1.23 km/km^2) influences more to Moderate and Low Groundwater Potential Zones (Fig. 16(d)) because this class covers the both of Zones largely than the other drainage density classes. The agriculture and bare land class of LULC effect the Moderate and Low Groundwater Potential zones respectively (Fig. 16(e)) because agriculture covers the most of study region and allow the water to be percolate relative to bare land. The Soil classes, Loamy soil and Clayey loam soil influence the Moderate and Low Groundwater Potential Zones (Fig. 16(f)) because Loamy soil has more porosity and permeability than clayey loam soil. The NDVI classes such as (0.13–0.16) and (0.08–0.13) has more efficacy to Moderate and Low Groundwater Potential Zones (Fig. 16(g)) respectively because 0.13–0.16 NDVI class allow more water to recharge the groundwater than 0.08–0.13 NDVI class. The 0–2 to 2–5 degree classes of Slope effect the Moderate to Low Groundwater Potential Zones (Fig. 16(h)) respectively because 0–2
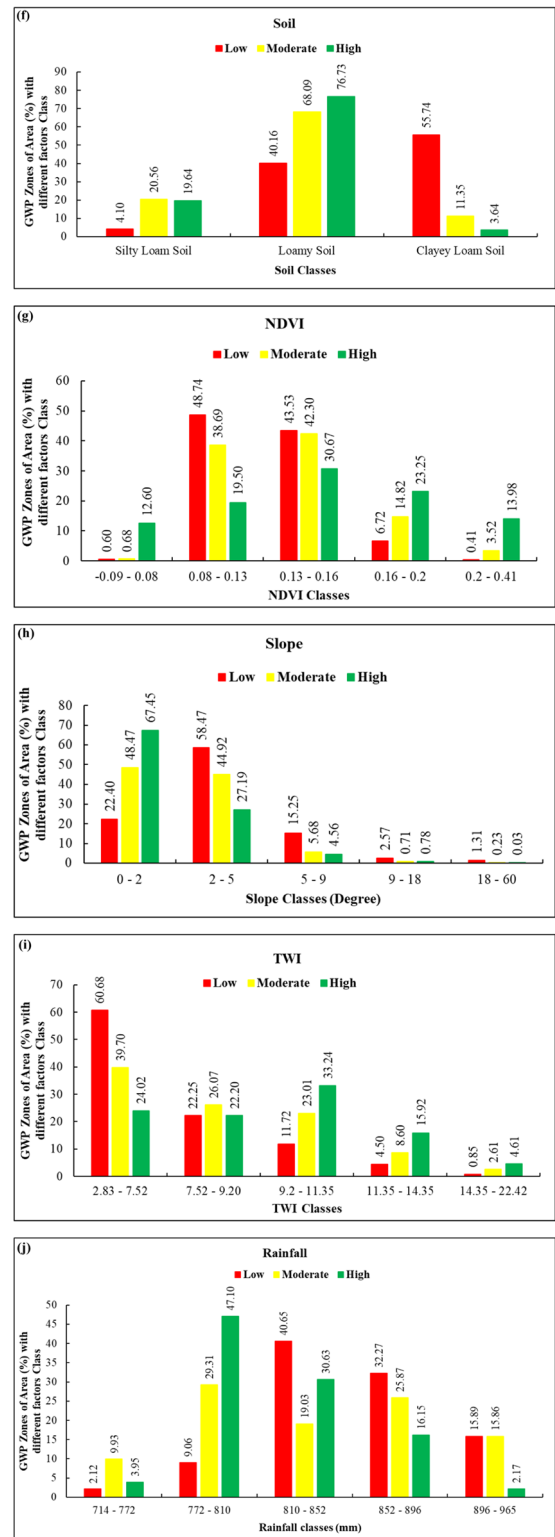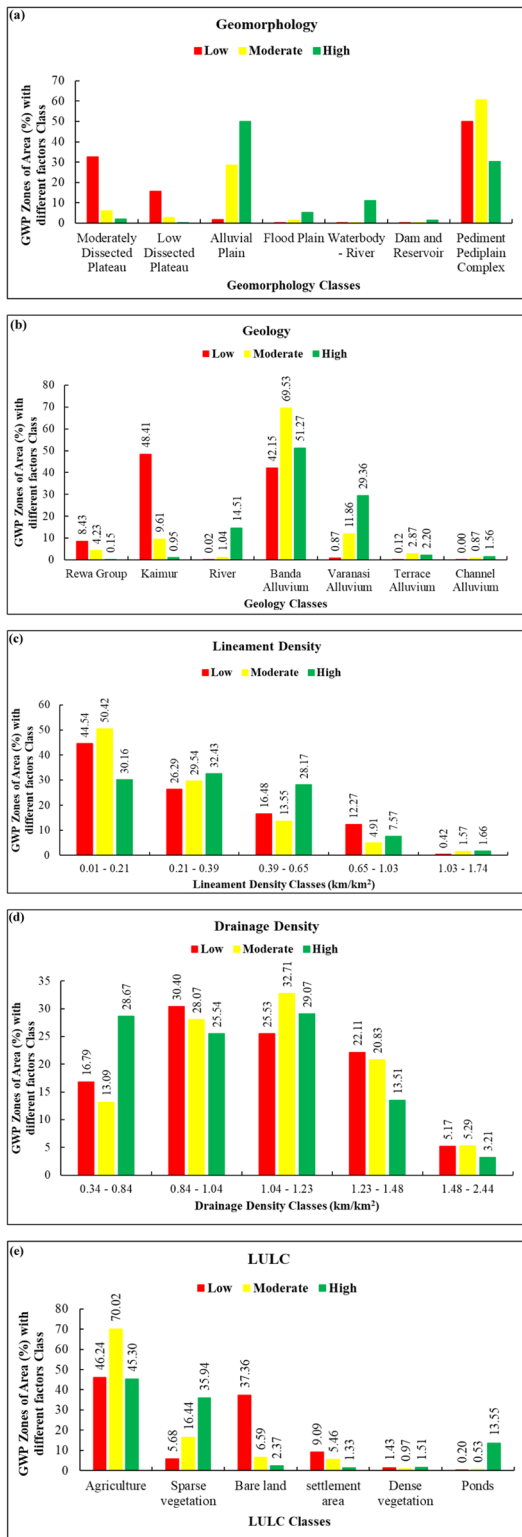
Fig. 16 (a to j): The relative influence of parameters classes on Groundwater Potential Zones

Fig. 16 (continued)

Table 10 Map removal sensitivity analysis statistics

Parameters	Standard Deviation
Geomorphology	5.6617
Geology	5.6917
LD	5.0951
DD	3.1178
LULC	1.8293
Soil	2.2161
NDVI	1.7838
Slope	2.6625
TWI	2.2093
Rainfall	2.8117

degree of slope restrain the surface water run – off than 2–5 degree class of Slope. The lower class 2.83–7.52 of TWI is responsible for the Moderate and Low Groundwater Potential Zones (Fig. 16(i)) The Rainfall classes, (772–810 mm) and (810–852 mm) shows large impact on Moderate and Low Groundwater Potential Zones (Fig. 16(j)) Respectively.

Although, by this map it can be predicted that the study region has the moderate Groundwater Potential Zones.

Map removal sensitivity analysis for groundwater potential zone

Map removal Sensitivity analysis evaluates the variability or unpredictability of model output result by assessing the consequences of removing individual thematic layers from the calculation of the groundwater potential map (Kindie et al., 2019; Thapa et al., 2018).

In this methodology, the approach involves removing each of the thematic layers individually and producing a new groundwater potential zone (GWZ) map by overlaying the remaining layers. Afterwards, the formula, which is utilized to compute a sensitivity
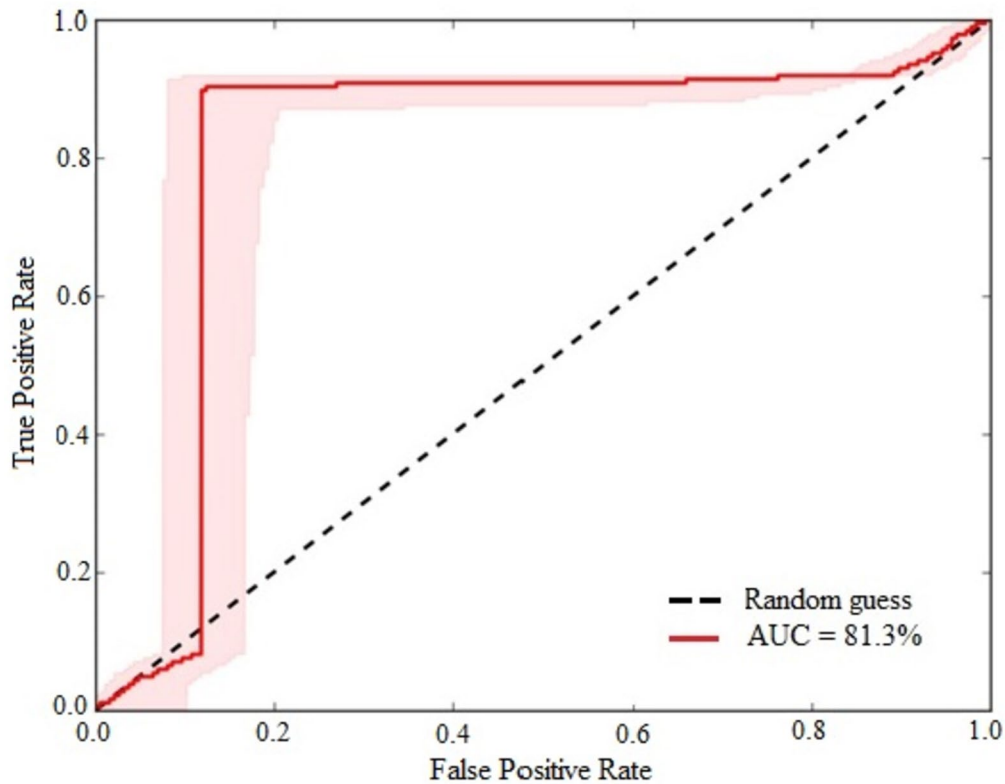

Fig. 17 ROC curve for validation of Groundwater Potential Zone

index, which serves to evaluate the influence of eliminating each layer, given as follows.

$$\text{SI} = \frac{\left| \frac{GPZ}{N} - \frac{GPZ'}{n} \right|}{GPZ} \times 100$$

SI denotes the sensitivity index for the removal of a single map, GWP represents the Groundwater Potential Index determined using all the thematic layers, and GWP' signifies the groundwater potential index computed by eliminating one thematic layer at a time. N and n represent the quantities of thematic layers utilized for computing GWP and GWP'.

The statistical findings from the map removal sensitivity analysis Table 10 indicate that the Geology and Geomorphology theme layers were the most important factors in estimating Groundwater Potential Zones. However, soil type, lineament density, drainage density, and rainfall were found to have a modest level of sensitivity.

After removing the Geological theme layer, the Geomorphology and Lineament density criteria gave higher variation index values. This shows that the lithology of the study area has a big effect on Groundwater Potential Zones.

Validation of outcome map prepared by AHP model

A statistical validation of the groundwater prospect map predictions was carried out in this study using a Receiver Operating Characteristic (ROC) curve (Nandi & Shakoor, 2010; Senapati & Das, 2021) by analysing with depth of water level in metres of 189 wells data using help of ArcSDM toolbox (www.sdmtoolbox.org). This toolbox needs to be added to ArcGIS software. This well data point was attained from the Bhuvan NRSC (https://bhuvan-app1.nrsc.gov.in/gwis/gwis.php#) site. These well's water level depth points were categorized as Good (<30 m), Moderate (30 – 80 m) and Poor (>80 m). These points were placed over the resulting map of GWPZ. In order to evaluate how accurate, the model is, the AUC value was determined to be between 0.5 and 1 (Manap et al., 2014; Naghibi et al., 2016). Being closer to the value 1 indicates that the model's accuracy is higher, whereas being closer to the value 0.5 indicates that the model's accuracy is lower. Although, the ROC curve predicted the authenticity

of this study was 81.3%. it suggests that the model performed very well (Fig. 17).

Conclusion

Groundwater is the main source of water for agriculture, domestic and industrial purposes in the Trans Yamuna region. Geospatial techniques with the aid of standard and remotely sensed geospatial data is effective in lessen the time, money, effort, and manpower, thus allowing for appropriate decision-making in regards to groundwater resource management and development. However, for the study region, the groundwater potential zones were determined through the application of an integrated remote sensing and GIS technique based on the AHP method. The outcome of the validation indicates that AHP is a credible method for determining the groundwater potential zones of the study area. The current study has a high level of scientific accuracy (accuracy = 81.3%) and may be helpful to the locals in selecting valuable well water drilling regions, as well as the authorities engaged in water resource management and land use planning. The study area exhibits an approximate 11.928% low zone of Groundwater potential and about 11.267% area is covered by the high Groundwater Potential Zone. Most of the area covered by the Moderate groundwater potential zone which is about 76.44% of the whole area. The final result is based on how each of the input parameters affected the AHP calculation. However, more discrepancies can be found between the final GPZ map and the well data for validation in the Koraon region than in any other region of study area. This region has sandstone rock, older alluvium, high to moderate Drainage Density and high rainfall.

Thus, large area of Koraon region has moderate groundwater potential zones and less area is covered by low groundwater potential zones. Preliminary Draft Report District Survey Report-Allahabad (In-Situ Rock, 2018) reports that groundwater flows in the Koraon region in north-west (high water table contour to low water table contour). Lineament trend is also in north-west direction and it is possible that same trend may exist in the subsurface. Therefore, the water table depth (mbgl) is greater in this region which is the cause of mismatch between

final GPZ map and well data for validation. According to this study, sustainable agricultural and economic development in the study region depends on prudent groundwater management. Rainwater harvesting and artificial recharge for the aquifer are needed to avoid the scarcity of water in the study region in the coming years. Plantation is needed in the Trans Yamuna region because it enhances the water holding capacity of the soil and allows the water to be infiltrate and it prevents the water run-off and erosion of the soil.

Author contribution (applicable for submissions with multiple authors)

Jayant Nath Tripathi: Conceptualized the problem, resources and supervision;

Swarnim and Irjesh Sonker: methodology and formal analysis, original draft preparation

Swarnim, Irjesh Sonker, Jayant Nath Tripathi and Surya Prakash Tiwari: writing—discussion, review and editing

All authors have read and agreed to the published version of the manuscript.

All authors have read, understood, and have complied as applicable w`ith the statement on "Ethical responsibilities of Authors" as found in the Instructions for Authors.

Data availability Data and material are given in the manuscript.

Declarations

Competing interests The authors declare no competing interests.

Conflict of interest The authors declare no competing interests.

References

Abdulkadir, T. S., Muhammad, R. U. M., Wan Yusof, K., Ahmad, M. H., Aremu, S. A., Gohari, A., & Abdurrasheed, A. S. (2019). Quantitative analysis of soil erosion causative factors for susceptibility assessment in a complex watershed. *Cogent Engineering*, *6*(1). https://doi.org/10.1080/23311916.2019.1594506

Agarwal, E., Agarwal, R., Garg, R. D., & Garg, P. K. (2013). Delineation of groundwater potential zone: An AHP/ANP approach. *Journal of Earth System Sciences, 122*(3), 887–898.

Al-Abadi, A. M., Al-Temmeme, A. A., & Al-Ghanimy, M. A. (2016). A GIS-based combining of frequency ratio and index of entropy approaches for mapping groundwater availability zones at Badra–Al Al-Gharbi–Teeb areas, Iraq. *Sustainable Water Resources Management, 2*(3), 265–283. https://doi.org/10.1007/s40899-016-0056-5

Alesheikh, A. A., & Hosseinali, F. (2008). Weighting Spatial Information in GIS for Copper Mining Exploration. *American Journal of Applied Sciences, 5*(9), 1187–1198.

Al-Fugara, A., Pourghasemi, H. R., Al-Shabeeb, A. R., Habib, M., Al-Adamat, R., Al-Amoush, H., & Collins, A. L. (2020). A comparison of machine learning models for the mapping of groundwater spring potential. *Environmental Earth Sciences*, *79*(10). https://doi.org/10.1007/s12665-020-08944-1

Allafta, H., Opp, C., & Patra, S. (2021). Identification of groundwater potential zones using remote sensing and GIS techniques: A case study of the shatt Al-Arab Basin. *Remote Sensing, 13*(1), 1–28. https://doi.org/10.3390/rs13010112

Antonio Alonso, J., & Teresa Lamata, M. (2006). Consistency in the Analytic Hierarchy Process: a new approach. *In International Journal of Uncertainty, Fuzziness and Knowledge-Based Systems*, *14*(4). www.worldscientific.com. Accessed 8 Jul 2023.

Arabameri, A., Pradhan, B., Pourghasemi, H. R., & Rezaei, K. (2018). Identification of erosion-prone areas using different multi-criteria decision-making techniques and gis. *Geomatics Natural Hazards and Risk, 9*(1), 1129–1155. https://doi.org/10.1080/19475705.2018.1513084

Arefin, R. (2020). Groundwater potential zone identification at Plio-Pleistocene elevated tract, Bangladesh: AHP-GIS and remote sensing approach. *Groundwater for Sustainable Development*, *10*. https://doi.org/10.1016/j.gsd.2020.100340

Arefin, R. (2020). Groundwater potential zone identification using an analytic hierarchy process in Dhaka City, Bangladesh. *Environmental Earth Sciences*, *79*(11). https://doi.org/10.1007/s12665-020-09024-0

Arulbalaji, P., Padmalal, D., & Sreelash, K. (2019). GIS and AHP Techniques Based Delineation of Groundwater Potential Zones: a case study from Southern Western Ghats, India. *Scientific Reports*, *9*(1). https://doi.org/10.1038/s41598-019-38567-x

Ballerine, C. (2017). Topographic Wetness Index Urban Flooding Awareness Act Action Support.*Will and DuPage Counties, Illinois*.

Bera, A., Mukhopadhyay, B. P., & Barua, S. (2020). Delineation of groundwater potential zones in Karha river basin, Maharashtra, India, using AHP and geospatial techniques. *Arabian Journal of Geosciences*, *13*(15). https://doi.org/10.1007/s12517-020-05702-2

Berhanu, B., Melesse, A. M., & Seleshi, Y. (2013). GIS-based hydrological zones and soil geo-database of Ethiopia.

Catena, 104, 21–31. https://doi.org/10.1016/j.catena.2012.12.007

Beven, K. (1997). TOPMODEL: A critique. *Hydrological Processes, 11*(9), 1069–1085. https://doi.org/10.1002/(SICI)1099-1085(199707)11:9%3c1069::AID-HYP545%3e3.0.CO;2-O

Biju, C., Saktivel, R., Matheswaran, S., Akhila, P., & Rajkumar, P. (2018). Application of Analytic Hierarchy Process (AHP) in Groundwater Potential Mapping Using Remote Sensing and GIS in Nagavathi Sub-Basin, Tamil Nadu India. *JASC: Journal of Applied Science and Computations, 5*(9), 744.

Biswas, A., Arkoprovo, B., Adarsa, J., & Prakash, S. S. (2012). Delineation of Groundwater potential zones using Remote Sensing and Geographic Information System Techniques: A case study from Ganjam district, Orissa Delineation of Groundwater Potential Zones using Satellite Remote Sensing and Geographic Information System Techniques: A Case study from Ganjam district, Orissa, India. In *Research Journal of Recent Sciences*, *1*(9). www.isca.in. Accessed 13 Nov 2022.

Blachowski, J. (2016). Application of GIS spatial regression methods in assessment of land subsidence in complicated mining conditions: Case study of the Walbrzych coal mine (SW Poland). *Natural Hazards, 84*(2), 997–1014. https://doi.org/10.1007/s11069-016-2470-2

Boughariou, E., Allouche, N., Ben Brahim, F., Nasri, G., & Bouri, S. (2021). Delineation of groundwater potentials of Sfax region, Tunisia, using fuzzy analytical hierarchy process, frequency ratio, and weights of evidence models. *Environment, Development and Sustainability, 23*(10), 14749–14774. https://doi.org/10.1007/s10668-021-01270-x

Castillo, J. L. U., Cruz, D. A. M., Leal, J. A. R., Vargas, J. T., Tapia, S. A. R., & Celestino, A. E. M. (2022). Delineation of Groundwater Potential Zones (GWPZs) in a Semi-Arid Basin through Remote Sensing, GIS, and AHP Approaches. *Water (Switzerland)*, *14*(13). https://doi.org/10.3390/w14132138

Census (2011). https://www.census2011.co.in/census/district/546-allahabad.html

CGWB. (2021). *National Compilation on Dynamic Ground Water Resources of India, 2020.* http://cgwb.gov.in/GW-Assessment/GWRA-2017-National-Compilation.pdf

Chen, W., Peng, J., Hong, H., Shahabi, H., Liu, J., Zhu, A.-X., Pei, X., & Duan, Z. (2018). *Landslide susceptibility modelling using GIS-based machine learning techniques for Chongren County, Jiangxi Province, China.*

Chowdhury, A., Jha, M. K., Chowdary, V. M., & Mal, B. C. (2008). Integrated remote sensing and GIS-based approach for assessing groundwater potential in West Medinipur district, West Bengal, India. *International Journal of Remote Sensing, 30*(1), 231–250. https://doi.org/10.1080/01431160802270131

Dar, T., Rai, N., & Bhat, A. (2021). Delineation of potential groundwater recharge zones using analytical hierarchy process (AHP). *Geology, Ecology, and Landscapes, 5*(4), 292–307. https://doi.org/10.1080/24749508.2020.1726562

Das, S., Gupta, A., & Ghosh, S. (2017). Exploring groundwater potential zones using MIF technique in semi-arid region:

A case study of Hingoli district, Maharashtra. *Spatial Information Research, 25*(6), 749–756. https://doi.org/10.1007/s41324-017-0144-0

Das, S., & Pardeshi, S. D. (2018). Integration of different influencing factors in GIS to delineate groundwater potential areas using IF and FR techniques: a study of Pravara basin, Maharashtra, India. *Applied Water Science*, *8*(7). https://doi.org/10.1007/s13201-018-0848-x

Dhinsa, D., Tamiru, F., & Tadesa, B. (2022). Groundwater potential zonation using VES and GIS techniques: A case study of Weserbi Guto catchment in Sululta, Oromia, Ethiopia. *Heliyon*, *8*(8). https://doi.org/10.1016/j.heliyon.2022.e10245

Doke, A. B., Zolekar, R. B., Patel, H., & Das, S. (2021). Geospatial mapping of groundwater potential zones using multi-criteria decision-making AHP approach in a hardrock basaltic terrain in India. *Ecological Indicators*, *127*. https://doi.org/10.1016/j.ecolind.2021.107685

Edet, A. E., Okereke, C. S., Esu, E. O., & Teme, S. C. (1998). Application of remote-sensing data to groundwater exploration: A case study of the Cross River State, southeastern Nigeria. In *Hydrogeology Journal*, *6*. Springer-Verlag Received.

Fetter (2001*).* Applied hydrology, 4th Edition.

Fitts, C. R. (2013). Groundwater. In *Groundwater Science* (pp. 1–22). Elsevier. https://doi.org/10.1016/B978-0-12-384705-8.00001-7

Ganapuram, S., Kumar, G. T. V., Krishna, I. V. M., Kahya, E., & Demirel, M. C. (2009). Mapping of groundwater potential zones in the Musi basin using remote sensing data and GIS. *Advances in Engineering Software, 40*(7), 506–518. https://doi.org/10.1016/j.advengsoft.2008.10.001

Gassama Jallow, A., Diongue, D. M. L., Emvoutou, C. H., Mama, D., & Faye, S. (2020). Groundwater Recharge Zone Mapping Using GIS-based Analytical Hierarchy Process and Multi-Criteria Evaluation: Case Study of Greater Banjul Area. *American Journal of Water Resources, 8*(4), 182–190. https://doi.org/10.12691/ajwr-8-4-4

Gnanachandrasamy, G., Zhou, Y., Bagyaraj, M., Venkatramanan, S., Ramkumar, T., & Wang, S. (2018). Remote Sensing and GIS Based Groundwater Potential Zone Mapping in Ariyalur District, Tamil Nadu. *Journal of the Geological Society of India, 92*(4), 484–490. https://doi.org/10.1007/s12594-018-1046-z

Gorsevski, P. V., Gessler, P. E., Foltz, R. B., & Elliot, W. J. (2006). Spatial prediction of landslide hazard using logistic regression and ROC analysis. *Transactions in GIS, 10*(3), 395–415. https://doi.org/10.1111/j.1467-9671.2006.01004.x

Guisan, A., Weiss, S. B., & Weiss, A. D. (1999). GLM versus CCA spatial modelling of plant species distribution. In *Plant Ecology*, *143*.

Guru, B., Seshan, K., & Bera, S. (2017). Frequency ratio model for groundwater potential mapping and its sustainable management in cold desert, India. *Journal of King Saud University - Science, 29*(3), 333–347. https://doi.org/10.1016/j.jksus.2016.08.003

Han, L., Liu, Z., Ning, Y., & Zhao, Z. (2018). Extraction and analysis of geological lineaments combining a DEM

and remote sensing images from the northern Baoji loess area. *Advances in Space Research, 62*(9), 2480–2493. https://doi.org/10.1016/j.asr.2018.07.030

Hasanuzzaman, M., Mandal, M. H., Hasnine, M., & Shit, P. K. (2022). Groundwater potential mapping using multi-criteria decision, bivariate statistic and machine learning algorithms: evidence from Chota Nagpur Plateau, India. *Applied Water Science, 12*(4). https://doi.org/10.1007/s13201-022-01584-9

Ifediegwu, S. I. (2022). Assessment of groundwater potential zones using GIS and AHP techniques: a case study of the Lafia district, Nasarawa State, Nigeria. *Applied Water Science, 12*(1). https://doi.org/10.1007/s13201-021-01556-5

Islami, F. A., Tarigan, S. D., Wahjunie, E. D., & Dasanto, B. D. (2022). Accuracy Assessment of Land Use Change Analysis Using Google Earth in Sadar Watershed Mojokerto Regency. *IOP Conference Series: Earth and Environmental Science, 950*(1). https://doi.org/10.1088/1755-1315/950/1/012091

Israil, M., Al-hadithi, M., & Singhal, D. C. (2006). Application of a resistivity survey and geographical information system (GIS) analysis for hydrogeological zoning of a piedmont area, Himalayan foothill region, India. *Hydrogeology Journal, 14*(5), 753–759. https://doi.org/10.1007/s10040-005-0483-0

Jaiswal, R. K., Mukherjee, S., Krishnamurthy, J., & Saxena, R. (2003). Role of remote sensing and GIS techniques for generation of groundwater prospect zones towards rural development - An approach. *International Journal of Remote Sensing, 24*(5), 993–1008. https://doi.org/10.1080/01431160210144543

Jal-shakti. (2020). Extraction of Groundwater, *Ministry of Jal Shakti*.

Jasrotia, A. S., Kumar, A., & Singh, R. (2016). Integrated remote sensing and GIS approach for delineation of groundwater potential zones using aquifer parameters in Devak and Rui watershed of Jammu and Kashmir, India. *Arabian Journal of Geosciences, 9*(4). https://doi.org/10.1007/s12517-016-2326-9

Kabeto, J., Adeba, D., Regasa, M. S., & Leta, M. K. (2022). Groundwater Potential Assessment Using GIS and Remote Sensing Techniques: Case Study of West Arsi Zone, Ethiopia. *Water (Switzerland), 14*(12). https://doi.org/10.3390/w14121838

Kafi, K. M., Shafri, H. Z. M., & Shariff, A. B. M. (2014). An analysis of LULC change detection using remotely sensed data; A Case study of Bauchi City. *IOP Conference Series: Earth and Environmental Science, 20*(1). https://doi.org/10.1088/1755-1315/20/1/012056

Kaliraj, S., Chandrasekar, N., & Magesh, N. S. (2014). Identification of potential groundwater recharge zones in Vaigai upper basin, Tamil Nadu, using GIS-based analytical hierarchical process (AHP) technique. *Arabian Journal of Geosciences, 7*(4), 1385–1401. https://doi.org/10.1007/s12517-013-0849-x

Kim, J. C., Jung, H. S., & Lee, S. (2019). Spatial mapping of the groundwater potential of the Geum River basin using ensemble models based on remote sensing images. *Remote Sensing, 11*(19). https://doi.org/10.3390/rs11192285

Kindie, A. T., Enku, T., Moges, M. A., Geremew, B. S., & Atinkut, H. B. (2019). Spatial analysis of groundwater potential using gis based multi criteria decision analysis method in Lake Tana Basin, Ethiopia. *Lecture Notes of the Institute for Computer Sciences, Social-Informatics and Telecommunications Engineering, LNICST, 274*, 439–456. https://doi.org/10.1007/978-3-030-15357-1_37

Kumar, A., & Krishna, A. P. (2018). Assessment of groundwater potential zones in coal mining impacted hard-rock terrain of India by integrating geospatial and analytic hierarchy process (AHP) approach. *Geocarto International, 33*(2), 105–129. https://doi.org/10.1080/10106049.2016.1232314

Kumar, M., Sharma, K. K., Lal, D., Atul, Imam, A., & Suryavanshi, S. (2018). Identifying Prospective Areas for Groundwater Potential Zone in Allahabad City. *Journal of Environmental Nanotechnology, 7*(4), 16–24. https://doi.org/10.13074/jent.2018.12.184336

Kumar Dinkar, G., Singh, V., Dinkar, G. K., Farooqui, S. A., Singh, V. K., Verma, A. K., & Prabhat, P. (2019). Geology of South and Southwest part of Uttar Pradesh and its Mineral Significance Geodynamic Evolution of Bundelkhand craton, India View project Geodynamic Evolution of Bundelkhand Craton and Garhwal Himalaya View project Geology of South and Southwest part of Uttar Pradesh and its Mineral Significance. https://doi.org/10.25299/jgeet.2019.4.2-2.2441

Kumar, M., Singh, S. K., Kundu, A., Tyagi, K., Menon, J., Frederick, A., Raj, A., & Lal, D. (2022). GIS-based multi-criteria approach to delineate groundwater prospect zone and its sensitivity analysis. *Applied Water Science, 12*(4). https://doi.org/10.1007/s13201-022-01585-8

Lakshmi, S., V., Vinay, L. Y., & Reddy, K. (2018). Identification of groundwater potential zones using gis and remote sensing. *International Journal of Pure and Applied Mathematics, 119*(17), 3195–3210. http://www.acadpubl.eu/hub/. Accessed 14 Nov 2022

le Page, M., Berjamy, B., Fakir, Y., Bourgin, F., Jarlan, L., Abourida, A., Benrhanem, M., Jacob, G., Huber, M., Sghrer, F., Simonneaux, V., & Chehbouni, G. (2012). An Integrated DSS for Groundwater Management Based on Remote Sensing. The Case of a Semi-arid Aquifer in Morocco. *Water Resources Management, 26*(11), 3209–3230. https://doi.org/10.1007/s11269-012-0068-3

Magesh, N. S., Chandrasekar, N., & Soundranayagam, J. P. (2011). Morphometric evaluation of Papanasam and Manimuthar watersheds, parts of Western Ghats, Tirunelveli district, Tamil Nadu, India: A GIS approach. *Environmental Earth Sciences, 64*(2), 373–381. https://doi.org/10.1007/s12665-010-0860-4

Magesh, N. S., Chandrasekar, N., & Soundranayagam, J. P. (2012). Delineation of groundwater potential zones in Theni district, Tamil Nadu, using remote sensing, GIS and MIF techniques. *Geoscience Frontiers, 3*(2), 189–196. https://doi.org/10.1016/j.gsf.2011.10.007

Mageshkumar, P., Subbaiyan, A., Lakshmanan, E., & Thirumoorthy, P. (2019). Application of geospatial techniques in delineating groundwater potential zones: a case study from South India. *Arabian Journal of Geosciences, 12*(5). https://doi.org/10.1007/s12517-019-4289-0

Mahato, R., Bushi, D., Nimasow, G., Dai Nimasow, O., Chandra Joshi, R., & Mahato, R. (2021). AHP and GIS-based Delineation of Groundwater Potential of Papumpare District of Arunachal Pradesh (India). https://doi.org/10.21203/rs.3.rs-350312/v1

Maity, B., Mallick, S. K., Das, P., & Rudra, S. (2022). Comparative analysis of groundwater potentiality zone using fuzzy AHP, frequency ratio and Bayesian weights of evidence methods. *Applied Water Science*, *12*(4). https://doi.org/10.1007/s13201-022-01591-w

Mallick, J., Singh, C. K., Al-Wadi, H., Ahmed, M., Rahman, A., Shashtri, S., & Mukherjee, S. (2015). Geospatial and geostatistical approach for groundwater potential zone delineation. *Hydrological Processes, 29*(3), 395–418. https://doi.org/10.1002/hyp.10153

Mallick, J., Alqadhi, S., Talukdar, S., Alsubih, M., Ahmed, M., Khan, R. A., Ben Kahla, N., & Abutayeh, S. M. (2021). Risk assessment of resources exposed to rainfall induced landslide with the development of gis and rs based ensemble metaheuristic machine learning algorithms. *Sustainability (Switzerland), 13*(2), 1–30. https://doi.org/10.3390/su13020457

Manap, M. A., Sulaiman, W. N. A., Ramli, M. F., Pradhan, B., & Surip, N. (2013). A knowledge-driven GIS modeling technique for groundwater potential mapping at the Upper Langat Basin, Malaysia. *Arabian Journal of Geosciences, 6*(5), 1621–1637. https://doi.org/10.1007/s12517-011-0469-2

Manap, M. A., Nampak, H., Pradhan, B., Lee, S., Sulaiman, W. N. A., & Ramli, M. F. (2014). Application of probabilistic-based frequency ratio model in groundwater potential mapping using remote sensing data and GIS. *Arabian Journal of Geosciences, 7*(2), 711–724. https://doi.org/10.1007/s12517-012-0795-z

Melese, T., & Belay, T. (2022). Groundwater Potential Zone Mapping Using Analytical Hierarchy Process and GIS in Muga Watershed, Abay Basin, Ethiopia. *Global Challenges, 6*(1), 2100068. https://doi.org/10.1002/gch2.202100068

Ministry of Environment Forest and Climate Change Notification. (2018). *District Survey Report. 7*(July), 29.

Moghaddam, D. D., Rezaei, M., Pourghasemi, H. R., Pourtaghie, Z. S., & Pradhan, B. (2015). Groundwater spring potential mapping using bivariate statistical model and GIS in the Taleghan Watershed, Iran. *Arabian Journal of Geosciences, 8*(2), 913–929. https://doi.org/10.1007/s12517-013-1161-5

Mohammady, M., Pourghasemi, H. R., & Pradhan, B. (2012). Landslide susceptibility mapping at Golestan Province, Iran: A comparison between frequency ratio, Dempster-Shafer, and weights-of-evidence models. *Journal of Asian Earth Sciences, 61*, 221–236. https://doi.org/10.1016/j.jseaes.2012.10.005

Moharir, K. N., Pande, C. B., Gautam, V. K., Singh, S. K., & Rane, N. L. (2023). Integration of hydrogeological data, GIS, and AHP techniques applied to delineate groundwater potential zones in sandstone, limestone, and shales rocks of the Damoh district, (MP) central India. *Environmental Research, 228*, 115832. https://doi.org/10.1016/j.envres.2023.115832

Mukherjee, P., Singh, C. K., & Mukherjee, S. (2012). Delineation of Groundwater Potential Zones in Arid Region of India-A Remote Sensing and GIS Approach. *Water Resources Management, 26*(9), 2643–2672. https://doi.org/10.1007/s11269-012-0038-9

Mukherjee, I., & Singh, U. K. (2020). Delineation of groundwater potential zones in a drought-prone semi-arid region of east India using GIS and analytical hierarchical process techniques. *Catena, 194*. https://doi.org/10.1016/j.catena.2020.104681

Muralitharan, J., & Palanivel, K. (2015). Groundwater targeting using remote sensing, geographical information system and analytical hierarchy process method in hard rock aquifer system, Karur district, Tamil Nadu, India. *Earth Science Informatics, 8*(4), 827–842. https://doi.org/10.1007/s12145-015-0213-7

Murmu, P., Kumar, M., Lal, D., Sonker, I., & Singh, S. K. (2019). Delineation of groundwater potential zones using geospatial techniques and analytical hierarchy process in Dumka district, Jharkhand, India. *Groundwater for Sustainable Development*, *9*. https://doi.org/10.1016/j.gsd.2019.100239

Murthy, K. S. R., & Mamo, A. G. (2009). Multi-criteria decision evaluation in groundwater zones identification in Moyale-Teltele subbasin, South Ethiopia. *International Journal of Remote Sensing, 30*(11), 2729–2740. https://doi.org/10.1080/01431160802468255

Naghibi, S. A., Pourghasemi, H. R., & Dixon, B. (2016). GIS-based groundwater potential mapping using boosted regression tree, classification and regression tree, and random forest machine learning models in Iran. *Environmental Monitoring and Assessment, 188*(1), 1–27. https://doi.org/10.1007/s10661-015-5049-6

Nandi, A., & Shakoor, A. (2010). A GIS-based landslide susceptibility evaluation using bivariate and multivariate statistical analyses. *Engineering Geology, 110*(1–2), 11–20. https://doi.org/10.1016/j.enggeo.2009.10.001

Narayanamurthi, V., & Ramasamy, A. (2022). Groundwater potential zoning by integrating multi-criteria decision and bivariate analysis methods–a case study on Cheyyar River Basin, Tamil Nadu, India. *Geocarto International*. https://doi.org/10.1080/10106049.2022.2088864

Narendra Modi, S. (n.d.). राष्ट्रीय जल मिशन *National Water Mission* जल संसाधन, नदी विकास और गंगा संरक्षण मंत्रालय *Ministry of Water Resources, River Development and Ganga Rejuvenation* भारत सरकार *Government of India A year of Inclusive Development in Water Resources sector...... Sushri Uma Bharati Minister for Water Resources, River Development and Ganga Rejuvenation Prof. Sanwar Lal Jat Minister of State for Water Resources, River Development and Ganga Rejuvenation.*

Oke, S. A. (2020). Regional aquifer vulnerability and pollution sensitivity analysis of DRASTIC: Application to Dahomey Basin of Nigeria. *International Journal of Environmental Research and Public Health, 17*(7), 2609. https://doi.org/10.3390/ijerph17072609

Owolabi, S. T., Madi, K., Kalumba, A. M., & Orimoloye, I. R. (2020). A groundwater potential zone mapping approach for semi-arid environments using remote sensing (RS), geographic information system (GIS), and analytical hierarchical process (AHP) techniques:

A case study of Buffalo catchment, Eastern Cape, South Africa. *Arabian Journal of Geosciences, 13*, 1184. https://doi.org/10.1007/s12517-020-06166-0/Published

Ozdemir, A. (2011). GIS-based groundwater spring potential mapping in the Sultan Mountains (Konya, Turkey) using frequency ratio, weights of evidence and logistic regression methods and their comparison. *Journal of Hydrology, 411*(3–4), 290–308. https://doi.org/10.1016/j.jhydrol.2011.10.010

Pande, C. B., Moharir, K. N., Panneerselvam, B., Singh, S. K., Elbeltagi, A., Pham, Q. B., Varade, A. M., & Rajesh, J. (2021). Delineation of groundwater potential zones for sustainable development and planning using analytical hierarchy process (AHP), and MIF techniques. *Applied Water Science, 11*(12). https://doi.org/10.1007/s13201-021-01522-1

Pandey, H. K., (2009). Ground water brochure of allahabad district, U.P., (A.A.P.: 2008–2009), pages 18.

Pant, S., Kumar, A., Ram, M., Klochkov, Y., & Sharma, H. K. (2022). Consistency Indices in Analytic Hierarchy Process: A Review. In *Mathematics*, *10*(8). MDPI. https://doi.org/10.3390/math10081206

Parizi, E., Hosseini, S. M., Ataie-Ashtiani, B., & Simmons, C. T. (2020). Normalized difference vegetation index as the dominant predicting factor of groundwater recharge in phreatic aquifers: case studies across Iran. *Scientific Reports*, *10*(1). https://doi.org/10.1038/s41598-020-74561-4

Park, I., Kim, Y., & Lee, S. (2014). Groundwater productivity potential mapping using evidential belief function. *Ground Water, 52*, 201–207. https://doi.org/10.1111/gwat.12197

Patra, S., Mishra, P., & Mahapatra, S. C. (2018). Delineation of groundwater potential zone for sustainable development: A case study from Ganga Alluvial Plain covering Hooghly district of India using remote sensing, geographic information system and analytic hierarchy process. *Journal of Cleaner Production, 172*, 2485–2502. https://doi.org/10.1016/j.jclepro.2017.11.161

Pinto, D., Shrestha, S., Babel, M. S., & Ninsawat, S. (2017). Delineation of groundwater potential zones in the Comoro watershed, Timor Leste using GIS, remote sensing and analytic hierarchy process (AHP) technique. *Applied Water Science, 7*(1), 503–519. https://doi.org/10.1007/s13201-015-0270-6

Pourghasemi, H. R., & Beheshtirad, M. (2015). Assessment of a data-driven evidential belief function model and GIS for groundwater potential mapping in the Koohrang Watershed, Iran. *Geocarto International, 30*(6), 662–685. https://doi.org/10.1080/10106049.2014.966161

Pourtaghi, Z. S., & Pourghasemi, H. R. (2014). GIS-based groundwater spring potential assessment and mapping in the Birjand Township, southern Khorasan Province, Iran. *Hydrogeology Journal, 22*(3), 643–662. https://doi.org/10.1007/s10040-013-1089-6

Preliminary Draft Report District Survey Report-Allahabad (In-situ Rock) Content. (2018).

Rajasekhar, M., Sudarsana Raju, G., & Siddi Raju, R. (2019). Assessment of groundwater potential zones in parts of the semi-arid region of Anantapur District, Andhra Pradesh, India using GIS and AHP approach. *Modelling Earth Systems and Environment, 5*(4), 1303–1317. https://doi.org/10.1007/s40808-019-00657-0

Rajesh, J., Pande, C. B., Kadam, S. A., Gorantiwar, S. D., & Shinde, M. G. (2021). Exploration of groundwater potential zones using analytical hierarchical process (AHP) approach in the Godavari River basin of Maharashtra in India. *Applied Water Science*, *11*(12). https://doi.org/10.1007/s13201-021-01518-x

Razandi, Y., Pourghasemi, H. R., Neisani, N. S., & Rahmati, O. (2015). Application of analytical hierarchy process, frequency ratio, and certainty factor models for groundwater potential mapping using GIS. *Earth Science Informatics, 8*(4), 867–883. https://doi.org/10.1007/s12145-015-0220-8

Rejith, R. G., Anirudhan, S., & Sundararajan, M. (2019). Delineation of groundwater potential zones in hard rock terrain using integrated remote sensing, GIS and MCDM techniques: A case study from vamanapuram river basin, Kerala, India. In *GIS and Geostatistical Techniques for Groundwater Science* (pp. 349–364). Elsevier. https://doi.org/10.1016/B978-0-12-815413-7.00025-0

Rossi, M., Bornaetxea, T., & Reichenbach, P. (2021). LAND-SUITE V1.0: a suite of tools for statistically-based landslide susceptibility zonation. *Geoscientific Model Development*. 10.5194/gmd-2021-343

Saaty, T. L. (1980). *The Analytic Hierarchy Process*. McGraw-Hill.

Saaty, T. L. (1990). How to make a decision: The analytic hierarchy process. *European Journal of Operational Research, 48*(1), 9–26. https://doi.org/10.1016/0377-2217(90)90057-I

Saaty, T. L., & Vargas, L. G. (1980). Hierarchical analysis of behavior in competition: Prediction in chess. *Behavioral Science, 25*(3), 180–191. https://doi.org/10.1002/bs.3830250303

Saaty, T. L. (2008). Decision making with the analytic hierarchy process. In *International Journal of Services Sciences*, *1*(1).

Sadat-Noori, M., & Ebrahimi, K. (2016). Groundwater vulnerability assessment in agricultural areas using a modified DRASTIC model. *Environmental Monitoring and Assessment, 188*, 19. https://doi.org/10.1007/s10661-015-4915-6

Saha, S. (2017). Groundwater potential mapping using analytical hierarchical process: a study on Md. Bazar Block of Birbhum District, West Bengal. *Spatial Information Research, 25*(4), 615–626. https://doi.org/10.1007/s41324-017-0127-1

Saha, A. K., & Agrawal, S. (2020). Mapping and assessment of flood risk in Prayagraj district, India: a GIS and remote sensing study. *Nanotechnology for Environmental Engineering*, *5*(2). https://doi.org/10.1007/s41204-020-00073-1

Sar, N., Khan, A., Chatterjee, S., & Das, A. (2015). Hydrologic delineation of ground water potential zones using geospatial technique for Keleghai river basin, India. *Modelling Earth Systems and Environment*, *1*(3). https://doi.org/10.1007/s40808-015-0024-3

Saranya, T., & Saravanan, S. (2020). Groundwater potential zone mapping using analytical hierarchy process (AHP)

and GIS for Kancheepuram District, Tamilnadu, India. *Modelling Earth Systems and Environment, 6*(2), 1105–1122. https://doi.org/10.1007/s40808-020-00744-7

Sarmah, T., & Das, S. (2018). Urban flood mitigation planning for Guwahati: A case of Bharalu basin. *Journal of Environmental Management, 206*, 1155–1165. https://doi.org/10.1016/j.jenvman.2017.10.079

Satpathy, B. N., & Kanungo, D. N. (1976). Groundwater exploration in hard-rock terrain-a case history. *Geophysical Prospecting, 24*, 725–776.

Scanlon, B. R., Reedy, R. C., Stonestrom, D. A., Prudic, D. E., & Dennehy, K. F. (2005). Impact of land use and land cover change on groundwater recharge and quality in the southwestern US. *Global Change Biology, 11*(10), 1577–1593. https://doi.org/10.1111/j.1365-2486.2005.01026.x

Senapati, U., & Das, T. K. (2022). GIS-based comparative assessment of groundwater potential zone using MIF and AHP techniques in Cooch Behar district, West Bengal. *Applied Water Science*, *12*(3). https://doi.org/10.1007/s13201-021-01509-y

Senapati, U., & Das, T. K. (2021). Assessment of basin-scale groundwater potentiality mapping in drought-prone upper Dwarakeshwar River basin, West Bengal, India, using GIS-based AHP techniques. *Arab Journal of Geosciences, 14*, 960. https://doi.org/10.1007/s12517-021-07316-8

Shukla, S. M. (2014). Spatial Analysis for Groundwater Potential Zones using GIS and Remote Sensing in the Tons Basin of Allahabad District, Uttar Pradesh, (India). *Proceedings of the National Academy of Sciences India Section A - Physical Sciences, 84*(4), 587–593. https://doi.org/10.1007/s40010-014-0157-1

Sikdar, P. K. (2018). Groundwater development and management: Issues and challenges in South Asia. *Groundwater Development and Management: Issues and Challenges in South Asia*, *January*, 1–539. https://doi.org/10.1007/978-3-319-75115-3

Singh, S., & Srivastava, R. (2011). Geology of Allahabad (India) and assessment of recharge for sustainability. *Proceedings of Indian Geotechnical Conference*, 15–17.

Sonwane, K., & Ullah Usmani, H. (2021). Assessment of Groundwater Potential Zones Using Geographic Information System and Analytic Hierarchy Process (AHP) Techniques in Chhoti Kali Sindh Watershed in Ujjain district, Madhya Pradesh, India. *Journal of Science and Technology, 06*, 122–131. https://doi.org/10.46243/jst.2021.v6.i05.pp122-131

Syed Wamiq Ali, Q., Lal, D., Jafri Ahsan, M., & Qazi Syed Wamiq Ali, C. (2015). *Impact Factor: 5.2 IJAR. 1*(13), 586–591. www.allresearchjournal.com. Accessed 21 Sept 2023

Taylor, R. G., Scanlon, B., Döll, P., Rodell, M., van Beek, R., Wada, Y., Longuevergne, L., Leblanc, M., Famiglietti, J. S., Edmunds, M., Konikow, L., Green, T. R., Chen, J., Taniguchi, M., Bierkens, M. F. P., Macdonald, A., Fan, Y., Maxwell, R. M., Yechieli, Y., & Treidel, H. (2013). Ground water and climate change. *Nature Climate Change, 3*(4), 322–329. https://doi.org/10.1038/nclimate1744

Thapa, R., Gupta, S., Guin, S., & Kaur, H. (2018). Sensitivity analysis and mapping the potential groundwater vulnerability zones in Birbhum district, India: A comparative approach between vulnerability models. *Water Science, 32*(1), 44–66. https://doi.org/10.1016/j.wsj.2018.02.003

Tiwari, V. (2018). Mapping Groundwater Potential Zones in Meja Block, Allahabad District Using Remote Sensing and GIS Techniques. *International Journal of Pure & Applied Bioscience, 6*(5), 573–583. https://doi.org/10.18782/2320-7051.6898

Todd. (2005). Groundwater hydrology, 3rd Edition.

Tolche, A. D. (2021). Groundwater potential mapping using geospatial techniques: A case study of Dhungeta-Ramis sub-basin, Ethiopia. *Geology, Ecology, and Landscapes, 5*(1), 65–80. https://doi.org/10.1080/24749508.2020.1728882

Unesco, (2020). World Water Assessment Programme (United Nations), & UN-Water. *Water and climate change*.

Vaux, H. (2011). Groundwater under stress: The importance of management. *Environmental Earth Sciences, 62*(1), 19–23. https://doi.org/10.1007/s12665-010-0490-x

Verma, N., & Patel, R. K. (2021). Delineation of groundwater potential zones in lower Rihand River Basin, India using geospatial techniques and AHP. *Egyptian Journal of Remote Sensing and Space Science, 24*(3), 559–570. https://doi.org/10.1016/j.ejrs.2021.03.005

Waikar M.L. & Nilawar, A. P. (2014). Identification of Groundwater Potential Zone using Remote Sensing and GIS Technique. In International Journal of Innovative Research in Science, Engineering and Technology, 3 (5), (An ISO 3297:2007). http://www.ijirset.com. Accessed 1 Oct 2021.

Yeh, H. F., Cheng, Y. S., Lin, H. I., & Lee, C. H. (2016). Mapping groundwater recharge potential zone using a GIS approach in Hualian River, Taiwan. *Sustainable Environment Research, 26*(1), 33–43. https://doi.org/10.1016/j.serj.2015.09.005

Zhang, Q., Zhang, S., Zhang, Y., Li, M., Wei, Y., Chen, M., Zhang, Z., & Dai, Z. (2021). GIS-based groundwater potential assessment in varied topographic areas of Mianyang city, Southwestern China, using AHP. *Remote Sensing, 13*(22). https://doi.org/10.3390/rs13224684